THE RELATIVE ION CURRENT TECHNIQUE FOR MASS SPECTROMETRIC MEASUREMENTS OF THE THERMODYNAMIC PROPERTIES OF MOLTEN ALLOYS

by

Jerry. L. Blattner

ProQuest LLC.
789 East Eisenhower Parkway
P.O. Box 1346
Ann Arbor, MI 48106 – 1346

T-1891

A Thesis submitted to the Faculty and the Board of Trustees of the Colorado School of Mines in partial fulfillment of the requirements for the degree of Doctor of Philosophy in Metallurgy.

Signed: Jerry L. Blattner

Jerry L. Blattner

Approved: J. P. Hager

J. P. Hager
Thesis Advisor

William M. Mueller

W. M. Mueller
Head, Department of
Metallurgical Engineering

Golden, Colorado

Date: November 9, 1976

ABSTRACT

A time-of-flight mass spectrometer fitted with a Knudsen cell inlet was used for the characterization and application of the relative ion current technique for activity and second law partial molar heat of mixing determinations of liquid metallic systems. This technique uses the ratio of the ion intensity of a pure reference metal at its melting point and the ion intensity of the alloy component of interest to eliminate variations in the cell and instrument parameters. This technique has special application as it can be used to define the thermodynamics of a single element of a multicomponent system. It is also applicable to narrow composition ranges thus eliminating the composition restriction of the normally used Knudsen cell-mass spectrometer method, the ion current ratio technique.

The magnitude and sensitivity of the error in the relative ion current method were investigated for various adjustable parameters and uncertainties of measurements. This study indicated that an error of less than 5% is easily obtained for the activity determinations. Errors in the partial molar heats of mixing were found to be very dependent upon the width of the temperature range studied and the uncertainty of the ion intensities measured. This error was shown to be of the

order of 30% or larger.

The relative ion current technique was used to study a single component of four binary alloys: Cu-In, Cu-Ga, Cu-Si, and Sn-Si. The activities and partial molar heats of mixing of the second component were calculated by the integration of the alpha and beta functions.

TABLE OF CONTENTS

LIST OF FIGURES

PAGE

PAGE

LIST OF TABLES

LIST OF APPENDICES

ACKNOWLEDGEMENTS

The author sincerely thanks Dr. J. P. Hager for his guidance and support during the course of his studies. Gratitude is expressed to the American Smelting and Refining Company for their support of the author under a fellowship grant.

The author is greatly indebted to his friends, both students and faculty, for the moral encouragement and interest they provided. Special gratitude is due to Mr. Bruce Schiller and Mr. W. Scott Moser for their time and friendship.

To the author's parents and family for their patience and affection during the difficult times the author is especially thankful.

I. INTRODUCTION

Although the fundamentals of the Knudsen cell-mass spectrometer system have been established for the past two decades its full development as a method for the study of alloy thermodynamics has only begun in recent years.[1] This recent interest has largely been due to the rapid expansion of the use of new materials and the need for fundamental data concerning production and characterization of these materials. The study presented here deals with the refinement and application of a new Knudsen cell-mass spectrometer method, the relative ion current technique, as initiated by S. M. Howard.[2,3] The two thermodynamic quantities determined by this technique are activities and partial molar heats of mixing. Specific discussion of these quantities and their uses can be found in references 4, 5, and 6.

An activity is defined for a species i, which occurs in the thermodynamic state α, by the following equation

$$\mu_i^{\alpha} - \mu_i^{o} \equiv RT \ln a_i^{\alpha} \qquad \text{(I-1)}$$

where

μ_i^{α} = chemical potential of i in the state α

μ_i^{o} = chemical potential of i in the standard state

a_i^α = activity of i in state α relative to i in the standard state

R = gas constant

T = temperature in degrees Kelvin.

Equation I-1 illustrates two important qualities of activities. First, activities are a function of their standard state, that is the value of an activity is relative to what is chosen as the standard state. The second characteristic shown by equation I-1 is that activities are comparisons of chemical potentials. Thus, activities are a measure of the differences of the potential chemical reactivity of a species under one set of conditions, state α, to that of a second set of conditions, standard state.

Activities are determined through their relationships to measurable intensive properties of the system. The expression of the relation used in Knudsen cell studies is that for ideal gases,

$$a_i^\alpha = \frac{P_i^\alpha}{P_i^o} a_i^o \qquad \text{(I-2)}$$

where

P_i^α = partial pressure of i in state α

P_i^o = partial pressure of i in standard state

a_i^α = activity of i in state α

a_i^o = activity of i in standard state.

This equation is used throughout this proposal.

The quantity used in relating composition to activity is the activity coefficient. The defining equation for this term is

$$\gamma_i = \frac{a_i}{C_i} \qquad \text{(I-3)}$$

where

C_i = an intensive expression of the concentration of i in the phase

a_i = activity of i in the phase at C_i

γ_i = activity coefficient of i at C_i .

The units of the concentration term are normally chosen to suit the system under investigation. Mole fraction X_i will be used for all systems in this proposal. A component is said to behave ideally if γ is unity, deviate negatively from ideality if γ is less than unity, and deviate positively from ideality if γ is greater than unity.

The temperature dependence of a_i is given by the partial molar enthalpy of mixing H_i^M, also called the relative partial molar enthalpy. The equation showing this dependence is

$$\ln a_{i,T_2} = \ln a_{i,T_1} + \frac{H_i^M}{R}\left(\frac{1}{T_2} - \frac{1}{T_1}\right) \qquad \text{(I-4)}$$

It is assumed in the above equation and throughout this thesis that the Kopp-Neumann rule[7] is applicable, $\Delta C_p = 0$.

Applications of Activities

The specific applications of activities are far too numerous to be given in this proposal. The following is a discussion of the three general areas of application.

Reaction Feasibility. Consider the reaction

$$A_{(g)} + B_{(l)} \rightarrow AB_{(s)} \qquad \text{(I-5)}$$

at constant T and P. The thermodynamic feasibility of the reaction is determined by the Gibb's free energy for the reaction,

$$\Delta G = \Delta G^{O} + RT \ln a_{AB}/(a_A \times a_B) \qquad \text{(I-6)}$$

where

ΔG^{O} = standard Gibb's free energy for the reaction

ΔG = Gibb's free energy for reaction.

If ΔG is negative, the reaction will proceed to the right; if positive, to the left; if zero, the system is at equilibrium.

The usefulness of equation I-6 lies in the fact that the quantities used in the equation can be calculated or measured without directly studying reaction I-5. Thus, thermodynamics allow the indirect investigation of systems which have not been previously studied or which are not amenable to direct investigation.

Reaction Equilibrium. The two general areas of reaction

equilibrium discussed here are the distribution between phases and extent of reaction.

Phase Distribution - Consider equation I-7 which describes a system of two phases at equilibrium containing a species i. At equilibrium the chemical potential of i must be the same for both phases.

$$\mu_i \text{ (Phase I)} = \mu_i \text{ (Phase II)} \qquad \text{(I-7)}$$

Substitution for μ_i by the defining equation for activity, equation I-1, results in an expression relating the activities of i in phases I and II,

$$\mu_i^* - \mu_i^o = RT \ln a_i^o(II) - RT \ln a_i^*(I) \qquad \text{(I-8)}$$

where

μ_i^* = chemical potential of i in the standard state *

μ_i^o = chemical potential of i in the standard state o

$a_i^*(I)$ = activity of i in phase I relative to state *

$a_i^o(II)$ = activity of i in phase II relative to state o.

Equation I-8 simplifies to equation I-9 for the case of identical standard states, $\mu_i^* = \mu_i^o$.

$$a_i(I) = a_i(II) \qquad \text{(I-9)}$$

Through the use of the definition of activity coefficients, equation I-9 can be arranged to form the commonly termed

distribution coefficient D.

$$\gamma_i^I X_i^I = \gamma_i^{II} X_i^{II}$$

$$\gamma_i^I / \gamma_i^{II} = X_i^{II} / X_i^I = D.$$

This ratio of activity coefficients has applications in solvent extraction and fractional distillation.

Extent of Reaction - The thermodynamic limit to which a reaction will proceed is determined by a ratio of equilibrium activities called the equilibrium constant K.

$$\Delta G^o = -RT \ln K$$

For the reaction

$$A + B \rightarrow AB,$$

the equilibrium constant is expressed as

$$K = a_{AB} / a_A \times a_B.$$

Through the use of the known quantities of K, a_{AB}, a_B and γ_A, the equilibrium concentration of A can be calculated,

$$X_A = a_{AB} / \gamma_A \times K \times a_B .$$

Although this example is greatly simplified, this is the basis for the thermodynamic prediction of reactor efficiency.[8]

Model Formulation and Evaluation. The chief difficulty

in the use of thermodynamics in process metallurgy is in obtaining accurate values of the quantities needed for calculations. At the present time a universal model for the prediction of activities and partial heats of mixing has not been developed. A number of models have been proposed but none are applicable to all metallic systems. Several of these models are the "quadric formalism" [9], the "zeroth order approximation theory" [10,11,12], the "sub-regular model" [13] and the "central-atoms model" [14].

The ultimate test for any model is the subjection of its predicted values to those experimentally determined. Thus, it is important that experimental data for a wide variety of systems be available for the evaluation of the limits of a model and to suggest further modifications.

Activity Measurements

Excellent descriptions of the prominant methods of activity determinations are given by Rapp[7] and Kubaschewski etal.[15] A brief description of the method used in this investigation and those used in the cited literature is given here. Partial molar heats of mixing are also determined by any of these methods as it is the temperature coefficient of activity. The methods discussed here are the galvanic cell, gas equilibrium, Knudsen effusion, and mass spectrometry.

Galvanic Cell. The galvanic cell measures the electrical

potential between the pure metal i and an alloy containing i.

$$i\ (\text{Pure}) = i\ (\text{Alloy})$$

An electrolyte is used to separate the metal and alloy while maintaining an ionic connection between them.

$$i\ (\text{Pure})\quad \text{electrolyte}\quad i\ (\text{Alloy})$$

The expressions for the activities and partial heats are

$$\ln a_i = \frac{nF}{RT} E$$

and

$$H_i^M = nF \frac{d(E/T)}{d(1/T)}$$

where

n = number of electrons in the reaction

$i\ (\text{Pure}) = i^{+n}\ (\text{electrolyte}) + ne^-$

F = Faraday's constant

E = potential of the cell.

The restrictions on the use of this method are:

1. the cell must never pass current
2. the electrolyte must be entirely ionic
3. the electrolyte must be inert with respect to i and the components of the alloy
4. the electrolyte must contain ions of i
5. the ions formed i^{+n} must all be of the same

oxidation state

6. the electrolyte must be an electronic insulator.

Gas Equilibrium. The gas equilibrium method utilizes a known equilibrium relationship of a reactive gas and a metal when the system is at equilibrium. Consider the reaction

$$A\ (gas) + B\ (alloy) = AB\ (solid).$$

The activities of the components of the above reaction are related by the equilibrium constant K.

$$K = \frac{a_{AB}}{a_A a_B}$$

Systems are generally chosen where the activity of AB is unity.

$$a_B = \frac{1}{a_A K}$$

The activity of B is determined by measuring the equilibrium pressure of A which is related to the activity of A by equation I-2.

$$a_A = \frac{P_A}{P_A^o}$$

$$a_B = \frac{P_A^o}{P_A K}$$

The restrictions on the application of the method are:

1. the activity of AB must be known
2. the equilibrium constant must be known
3. the alloy must be mutually insoluble with all other phases present
4. the equilibrium composition of the alloy must be known
5. the pressure of A must be accurately measured.

Knudsen Effusion. The pressure of a vapor species is utilized to determine the activity of the species in the condensed phase. The condensed phase is contained in the Knudsen cell. The cell is completely sealed except for a small orifice which allows a small portion of the equilibrium vapors to pass into the surrounding vacuum. The pressure of a vapor species i in the cell is related to the mass flux through the orifice by the Knudsen effusion equation.

$$P_i = \frac{1}{AK}\sqrt{\frac{2\pi RT}{M_i}}\ \frac{dW_i}{dt}$$

where

A = area of orifice

K = clausing factor for the orifice

M_i = molecular weight of i

$\frac{dW_i}{dt}$ = mass flux of i through the orifice.

The method of measuring the quantity $\frac{dW_i}{dt}$ is selected on the basis of the characteristics of vapor species. Consider a system where i forms only one vapor species and this

species is the only significant vapor produced by the condensed phase. Under these conditions the mass flux may be determined by sample weight loss, weight of condensed vapor, or analysis of force generated by the escaping vapors. If polymers and compounds of i are present in the gas phase, the complete analysis of the condensed vapor together with the thermodynamic relationships of the vapor species containing i must be determined.

Knudsen cells are used extensively in the studies presented in this paper. Further discussions of the properties of these devices are left to later chapters.

Restrictions to this technique are:

1. the sample composition must remain constant
2. the clausing factor and the orifice area must be known
3. all vapor species containing i must be known and the thermodynamic relation of each must be well established
4. the cell must be inert with respect to the sample
5. the gas and condensed phases must be at equilibrium.

Mass Spectrometry. The mass spectrometer is an analytical tool used to determine the composition of gases. This analysis is performed by separating the vapor species with respect to their masses and outputing a signal which is proportional to the partial pressure of each of the vapor species. The mass

spectrometer is therefore suitable for transpiration, gas equilibrium, and Knudsen effusion studies as a means of measuring equilibrium partial pressures. It is the application of the Knudsen cell - mass spectrometer system that is of interest here.

The effusing vapors from the Knudsen cell enter the mass spectrometer where they are ionized and then analyzed. The output for each of the vapor species in the effusate is a current, an ion current, which is related to the partial pressure of each species by

$$P_i = K_i \, I_i^+ \, T \qquad \text{(I-10)}$$

where

P_i = partial pressure of vapor species i

I_i^+ = ion current or ion intensity of species

T = cell temperature in degrees Kelvin

K_i = proportionality factor which is a function of cell geometry and orientation, machine parameters, and species characteristics.

The factor K_i is not a true constant as its parameters vary between experiments. Studies have been performed where K_i is evaluated and held constant. However, the restrictions of this approach are such that few alloy systems can be studied.

A more productive approach in using equation I-10 is the elimination of the variance of K_i through the use of ratios.

There are several methods for activity determinations based upon the use of ion current ratios. Two of these methods are described here.

Ion Current Ratio - The ion current ratio technique originated from the work done by Lyvbimov, Zobeus, and Rakhovski [16] and was further developed by Belton and Fruchen[17]. This method uses the ratio of the simultaneously measured ion intensities of two gas species produced by the sample in a Knudsen cell. Consider a binary alloy A-B. A study of the system A-B by mass spectrometry produces a set of ratios of ion currents of A to B for each temperature of each composition studied. The activity coefficients and partial heats of A are then determined by the graphic solution of the equations

$$\ln \gamma_{A\,X_A} = \int_{X_A=1}^{X_A=X_A} X_B \, d\ln \left[\frac{I_A^+ X_B}{I_B^+ X_A} \right] \qquad \text{(I-11)}$$

$$H_{A\,X_A}^{M} = -R \int_{X_A=1}^{X_A=X_A} X_B \, d \frac{d\ln(I_B^+/I_A^+)}{d(1/T)} \qquad \text{(I-12)}$$

where I_A^+ and I_B^+ are simultaneously measured ion currents of A and B at X_A and T. A similar set of equations is used to define the values for component B.

Multicomponent systems may also be investigated by this method. The study of these complex systems requires ion intensity measurements of each of the components throughout

the entire composition range of the system.

The restrictions of this technique are:

1. the ion currents of all components must be measurable over the entire composition range
2. the sample composition must remain constant throughout the run
3. the effusing vapors must be at equilibrium with the vapor over the sample
4. the cell must be inert with respect to the sample.

Restriction 1 above is very significant in the dilute composition regions. As the mole fraction of a component approaches zero the vapor pressure and the corresponding ion current of the component also approach zero. The errors involved in measuring these small quantities results in the instability in the ratios used in equations I-11 and I-12. The errors produced by this effect are especially significant when the vapor pressures of the components in the pure states differ by more than an order of magnitude.

Relative Ion Current - This is a new technique in the use of the Knudsen cell - mass spectrometer for thermodynamic studies which is the subject of this thesis. As in the ion current ratio method, ratios are made of two ion currents. This method, however, compares the ion current of the species of interest to the ion current of a reference metal held in a separate reference chamber of the Knudsen cell,

figure 1. The reference current is measured for each composition studied and is taken as the intensity arrest produced when the reference metal goes through a phase transition. The temperature and vapor pressure of the reference intensity are thus constants of all measurements. As is shown in Chapter II, the formation of this ratio eliminates the variations in K when the same cell, machine, and electronic parameters are used.

The relative ion current equation is

$$P_i = \frac{K_i}{K_r} \frac{P_r}{T_r} \frac{I_i^+}{I_r^+} T_i \qquad \text{(I-13)}$$

or

$$P_i = K_R R_i^+ T_i \qquad \text{(I-14)}$$

where

$R_i^+ = \frac{I_i^+}{I_r^+} \equiv$ relative ion current

$T_i =$ temperature at which I_i^+ was measured

$K_R = \frac{K_i}{K_r} \frac{P_r}{T_r} =$ constant for the species i, r, and cell geometry.

The relationship of the relative ion current and the activity of i is derived from equation I-2.

$$a_i = \frac{P_i}{P_i^o} a_i^{STD}$$

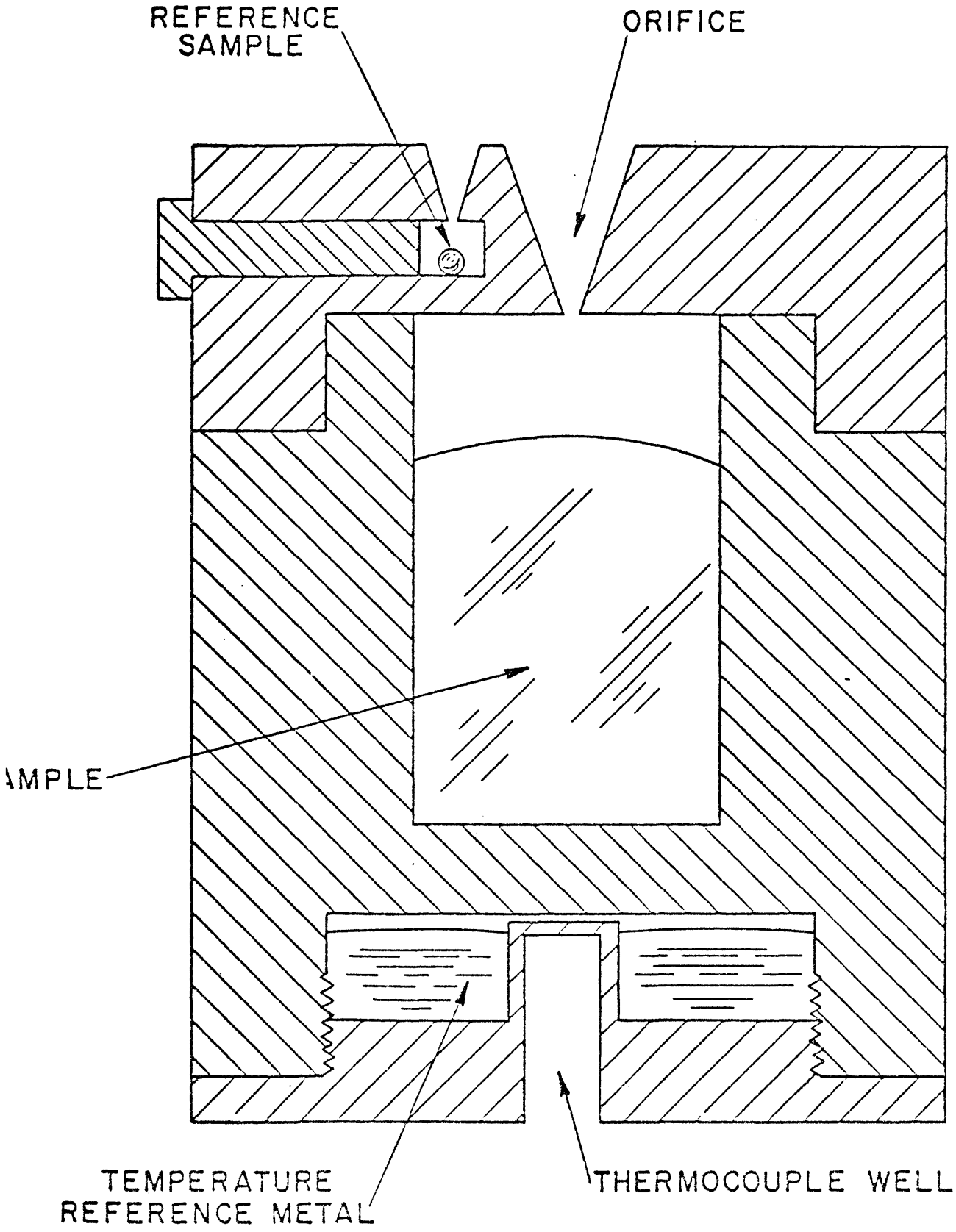

FIG. 1—GRAPHITE KNUDSEN CELL USED FOR THE RELATIVE ION-CURRENT MEASUREMENTS

$$a_i = \frac{K_R R_i^+ T_i}{K_R R_i^{+STD} T_i} \; a_i^{STD} = \frac{R_i^+}{R_i^{STD}} a_i^{STD} \qquad \text{(I-15)}$$

R_i^{+STD} is the relative ion current of i at T_i for some alloy for which the activity of i is known. The quotient of the relative ion currents of the alloy and the standard is termed the normalized relative ion current R_i^N . This definition is useful for three reasons: 1) ln R_i^N is a linear function of inverse temperature while ln R_i^+ is not, 2) In the case where the standard is the pure metal, R_i^N is equal to the activity, and 3) R_i^N is independent of the cell, machine and electronic parameters, R_i^+ is not.

The partial molar heats of mixing are determined by the slope of the plot of ln R_i^N against 1/T.

$$\ln R_i^N = \left(\frac{H_i^M - H_i^{M,STD}}{R}\right) \left(\frac{1}{T}\right) + K \qquad \text{(I-16)}$$

The advantages of this method over the ion current ratio are:

1. the activity of a species is determined by measuring the ion current of that specie only
2. the accuracy of the activity determination is not affected by differences in the partial pressures of the pure materials
3. there is no restriction on the compositions studied.

The restrictions for the application of the relative ion current are:

1. the ion intensity of the component of interest must be measurable; for the equipment used, the lowest quantitatively measurable pressure is of the order of 50 millipascals i.e. Ag at 1200^{o}K and Cu at 1400^{o}K.

2. the ion intensity of the component of interest must be determined for the pure element or for the element in a system for which the activity has been previously determined

3. the same cell must be used for measurements of R_i^+ and R_i^{+STD}

4. the composition of the sample must remain constant

5. the Knudsen cell must be inert with respect to the sample.

II. MATHEMATICAL FORMULATION

The relative ion current equation is developed in two parts: the formulation of the ion current equation I-10 and the derivation of the relative ion current equation I-15. This order of development is followed as an understanding of the ion current equation is necessary for the arguments involved in the relative ion expression derivation.

Ion Current Equation

The ion current is the product of two processes. These operations are the transport of a molecular beam from a chamber in the Knudsen cell to the ionization region of the mass spectrometer, and the conversion of the components of the beam to an ion current. A schematic of the total process is given in figure 2.

Molecular Beam. The Knudsen effusion equation [18,19] describes the flow rate of a vapor species i through a knife-edge orifice under molecular flow. This molar flow rate N_i is equal to the product of the flux ϕ_i of i striking the walls of the chamber and the area A_i of the chamber orifice. This rate is given by

$$N_i = \phi_i A_i = \tfrac{1}{4} \rho_i \bar{V}_i A_i$$

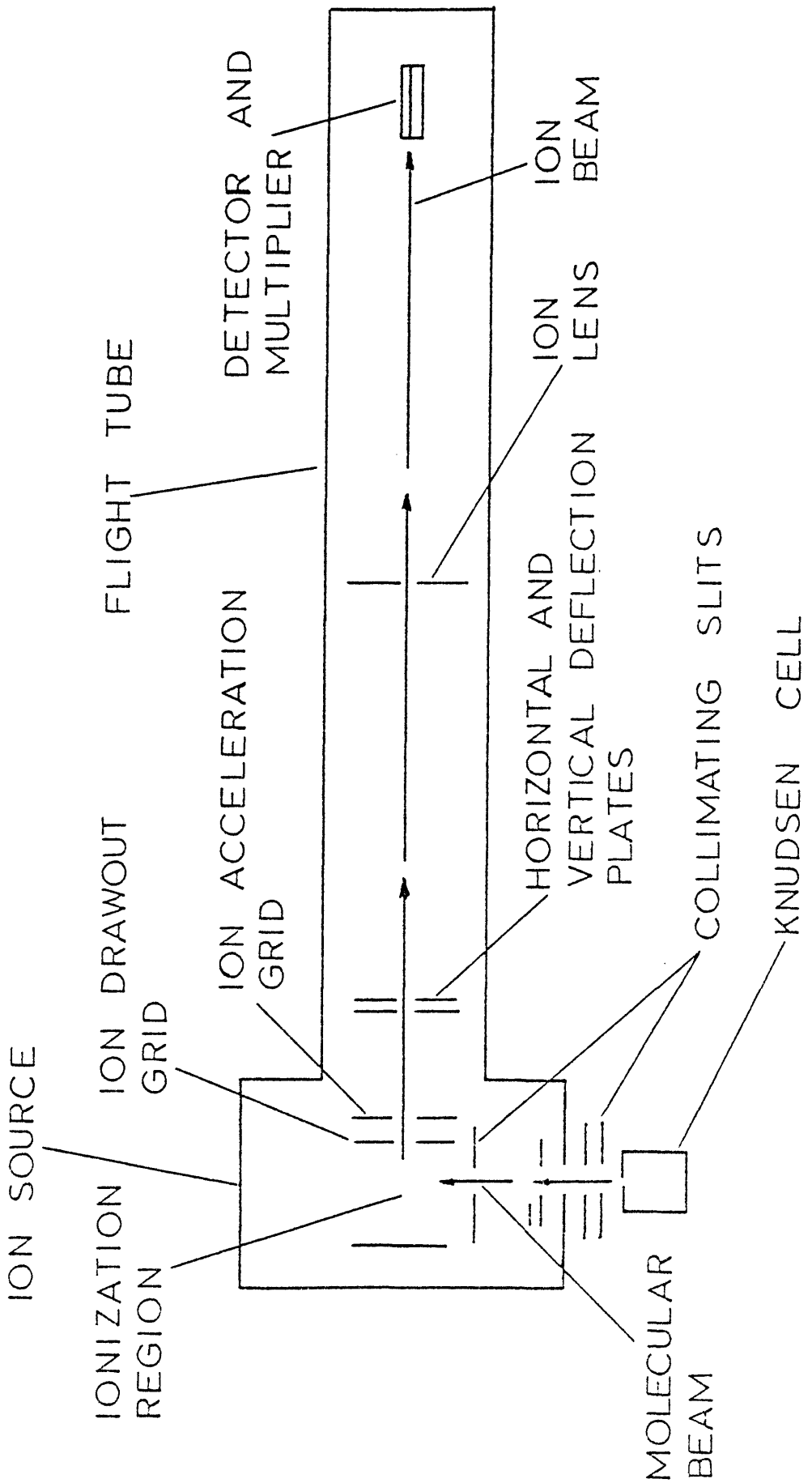

FIG. 2 — SCHEMATIC DIAGRAM OF THE KNUDSEN CELL — MASS SPECTROMETER SYSTEM.

where

$\bar{V}_i = \left[\frac{8RT}{\pi M_i}\right]^{\frac{1}{2}}$ - average velocity of i

$\rho_i = \frac{P_i n}{RT}$ - molecular density of i in the gas phase for an ideal gas

P_i = pressure of i

R = gas constant

n = Avogadro's number

T = absolute temperature

M_i = molecular weight of i.

When a knife-edge orifice is not used, a correction term, the clausing factor[18], is required. The clausing factor K_i is the ratio of the number of molecules leaving the orifice to the number of molecules incident to it. The general expression of the Knudsen equation is

$$N_i = A_i K_i P_i n (2\pi RT/M_i)^{-\frac{1}{2}} \qquad \text{(II-1)}$$

The distribution of the effusing gas will be isotropic within the confines of the orifice. Although the cosine distribution law [20,21] can be used to estimate the fraction of the effusate which enters the ion source, it is sufficient to state that the collimating slits select a fraction F_i of this molecular beam to pass into the ionization region. Therefore, the rate $N_{i,s}$ of molecules of species i entering the ionization region is given by

$$N_{i,s} = F_i A_i K_i P_i n (2\pi RT/M_i)^{-\frac{1}{2}} \quad \text{(II-2)}$$

Ion Current. There are three steps involved in the conversion of a gas to its ion current: (1) ionization of the gas, (2) transport of the ions to the detector, and (3) conversion of ions to electrical currents.

The reaction for the production of a singly charged species i^+ by electron impact is expressed as

$$I + e^- \rightarrow i^+ + 2e^-$$

The number of molecules of a specific isotope of i available for ionization N_i is determined by the isotopic abundance γ_i, depth L of the electron beam, the velocity of the molecules $\bar{V}_i$, and the rate of flux of molecules to the ionization region $N_{i,s}$.

$$N_i = N_{i,s} L \bar{V}_i^{-1} \gamma_i \quad \text{(II-3)}$$

For the above reaction to occur the electron must pass within the ionization cross section of the molecule. The ionization cross section σ_i is a function of the species i and the electron energy. The number of ions formed N_i^+ for a given electron energy is

$$N_{i+} = N_i \sigma_i N_e \alpha_i \quad \text{(II-4)}$$

where

N_e = number of electrons in electron beam

and

$$N_e = C\ t/q \qquad \text{(II-5)}$$

C = average ionization current

t = duration of one cycle

q = number of coulombs per ampere

α_i = ionization probability factor.

Once formed, these ions are accelerated by a potential drop towards the detector. Only a fraction f_i+ of the initial ions formed reach the detector.[22] This fraction is a constant for a given ionic species and a given set of electrical and geometric parameters for the mass spectrometer. The number of ions which reach the detector $N_i+,_D$ is

$$N_i+,_D = N_i+\ f_i+ \qquad \text{(II-6)}$$

The secondary electrons produced by the collision of an ion on the detector cathode is amplified by the multiplier to produce S_i^+ number of electrons. The total number of electrons produced by all the ions of i for a given number of analysis cycles is the ion current.

$$I_i^+ = S_i^+ N_{i,D}\ q/t \qquad \text{(II-7)}$$

Combining equations II-2 through II-7 and solving for P_i results in the expression

$$P_i = (4Rn^{-1})(A_iK_iF_i)^{-1}(LC)^{-1}(f_i^+\sigma_iS_i^+\alpha_i\gamma_i)I_i^+ T \qquad \text{(II-8)}$$

Using the indicated groupings of terms, the following definitions are made:

$K = 4Rn^{-1}$ = absolute constant

$G_i = (A_iK_iF_i)^{-1}$ = geometric term

$M_i = (LC)^{-1}$ = machine term

$S_i = (f_i^+\sigma_iS_i^+\alpha_i\gamma_i)^{-1}$ = species term.

The final form of the ion current equation is given by the substitution of these factors into equation II-8.

$$P_i = K\, G_i\, M_i\, S_i\, I_i^+ T \qquad \text{(II-9)}$$

Geometric Term - This product is solely a function of geometric considerations. The area of the Knudsen cell orifice A_i and its corresponding clausing factor K_i are constants for a given cell unless the orifice is altered by corrosion or cracking. The fraction of the effusing beam which enters the ion source F_i is dependent upon the position of the collimating slits and the Knudsen cell with respect to the ion source. This factor, a constant for a given experiment, may vary from one experiment to another.

Machine Term - The depth of the electron beam L is dependent upon positioning and strength of the collimating magnets, electron energy, and geometry of the ion source. These variables can be held constant for a series of experiments. The ionization current is monitored by the trap -

current, a sampling of C by a shielded cathode positioned opposite the electron gun. This trap current is held constant at a selected level by an electrometer - amplifier circuit which uses the trap current as an input signal. Therefore, C is a constant for a given trap current level.

Species Term - The ionization cross section σ_i of a given species is dependent solely upon the energy of the bombarding electrons. The design of the electron gun used in this work produces an electron energy distribution with a spread of several electron volts. The ionization cross section used in this term is therefore a weighted average of the cross sections corresponding to this energy distribution. The energy distribution is constant with 0.0 5 ev. thus maintaining a constant averaged σ_i for all experiments. The detector sensitivity, S_i^+, is a function of the secondary electron emission efficiency of the ion upon striking the detector cathode and the electrical and physical parameters of the multiplier[23]. For a specific ion this quantity is fixed over a series of experiments when these parameters are held constant. The fraction of the number of a specific ion formed in the ionization region which reach the detector f_i^+ is a function of the ion optics, ion acceleration potential, and geometries of the ion source and flight tube components. The acceleration potential and geometric factors are fixed for a set of experiments. A minimum and constant value of f_i^+ for a given analysis is obtained by maximizing the ion current through

the adjustment of the ion optics. It has been observed throughout the course of this experimental work that the settings for the ion optics which minimize f_i^+ are constants for a given ionic species. The probability of ionization of any one atom of the gas species in the ionization region α_i is a function of the density, energy, and duration of the electron beam and the geometry of the ion source. The geometric parameters of the source are constant. The characteristics of the electron beam can be fixed by using consistent trap current, electron energy, pulse time, and collimating magnet position for all measurements. Under these restraints α_i is constant for a given species for a complete set of experiments.

Relative Ion Current Equation

The relative ion current equation I-15 is formed by a ratio of two current expressions II-9. The first ion current expression is for the species i of interest which effused from the sample chamber of the Knudsen cell at temperature T.

$$P_i = K G_i M_i S_i I_i^+ T \qquad \text{(II-10)}$$

The second expression is for the reference metal r.

$$P_r = K G_r M_r S_r I_r^+ T_r \qquad \text{(II-11)}$$

The reference intensity I_r^+ is measured at the melting point of r so that both T_r and P_r are fixed. Forming the ratio and

multiplying by P_r gives the expression

$$P_i = \left(\frac{K}{K}\right)\left(\frac{G_i}{G_r}\right)\left(\frac{M_i}{M_r}\right)\left(\frac{S_i}{S_r}\right)\left(\frac{P_r}{T_r}\right)\left(\frac{I_i^+}{I_r^+}\right)T \qquad \text{(II-12)}$$

The product of the first five terms in equation II-12 is the relative ion current constant K_R .

$$K_R = \left(\frac{K}{K}\right)\left(\frac{G_i}{G_r}\right)\left(\frac{M_i}{M_r}\right)\left(\frac{S_i}{S_r}\right)\left(\frac{T_r}{P_r}\right)$$

Each of these terms and therefore K_R is equal to a true constant for each set of species i and r, Knudsen cell, and machine parameters as shown in the following arguments.

$$\frac{K}{K} = \frac{4Rn^{-1}}{4Rn^{-1}} = 1$$

This is the ratio of pure constants, the gas constant and Avogadro's number, and must equal unity for any experiment.

$$\frac{G_i}{G_r} = \frac{A_r K_r F_r}{A_i K_i F_i} = G = \text{constant}$$

The areas and the clausing factors of the sample and reference chamber orifices of a given cell are constants for any experiment. The ratio of these terms is therefore a constant for a given cell. The fractions of the effusing molecular beams which reach the ionization region F_i and F_r will individually change from experiment to experiment. These factors, however, are dependent solely upon the

geometry and the positioning with respect to the source and collimating slits of the respective orifices. As previously discussed, the orifice geometries are independent of the experiment. The experimental procedure of the technique, as outlined in Chapter V, is first the positioning of the reference orifice and then repositioning the cell so as to duplicate the reference orifice position with respect to the ion source and collimating slits with the sample orifice. This procedure produces a cancellation of any change in F_i between experiments by a proportional change in F_r. Thus, the ratio of F_i to F_r is a constant for a set of experiments using the same cell. As the ratios of each of the like terms of G are constants for a given cell then G must be a constant for a given cell.

$$\frac{M_i}{M_r} = \frac{L\ C}{L\ C} = 1$$

The depth of the electron beam is solely a function of the instrument's physical parameters which are held constant during an experiment. The average electron current C is held at a selected value throughout an experiment by setting the physical and electronic parameters, of which C is a function, at the beginning of a run and leaving these parameters undisturbed for the duration of the experiment. Therefore, L and C are identical for the sample and reference measurements made during any single study. The ratio of the machine parameters is equal to one for each experiment.

$$\frac{S_i}{S_r} = \frac{\alpha_r f_r^+ \sigma_r S_r^+ \gamma_r}{\alpha_i f_i^+ \sigma_i S_i^+ \gamma_i} = S = \text{constant}$$

The isotope of the species with the largest isotopic abundance is always used for the ion current measurements. The isotopic abundance for a given source of material is a constant. Thus, the ratio of γ_j is a constant for every run. The electron energy, geometry of ionization region, and ionization current are held constant for an entire set of experiments. The α_j and σ_j terms for both the reference and sample are constants under these afore mentioned constraints and therefore the ratios are equal to constants. The f_j^+ and S_j^+ terms are solely dependent upon the species j, the instrument's electronic parameters, and the geometries of the ion source, flight tube, and multiplier. As the electronics and geometries are fixed for a set of experiments the ratios of these terms for the reference and sample species is a constant. Each ratio of like terms in S are constants for a set of alloy measurements. Therefore, S is a constant for the same set.

$$\frac{P_r}{T_r} = \text{constant}$$

It can be shown through the phase rule that a system which consists of a single component in three phases has zero degrees of freedom, that is the temperature and pressure are fixed. This is the exact discription of the reference

metal at its fussion point. Therefore, T_r and P_r are constants for a specific metal r for all experiments.

Equation II-12 can therefore be simplified to the final form of the relative ion current equation for partial pressure of i

$$P_i = K_R R_i^+ T \qquad \text{(II-13)}$$

where

$$R_i^+ = \frac{I_i^+}{I_r^+}$$

K_r = constant for a given i, r, cell, and instrument parameters.

The activity of i for a given composition can thus be determined directly by equation II-15 which is developed by the substitution of equation II-13 into equation I-2.

$$a_i = \frac{K_R R_i^+ T}{K_R R_i^{STD} T} a_i^{STD} \qquad \text{(II-14)}$$

or

$$a_i = \frac{R_i^+}{R_i^{STD}} \quad a_i^{STD} = R_i^N a_i^{STD} \qquad \text{(II-15)}$$

The following derivation is for the equation relating the normalized relative ion currents to the partial molar heats of mixing. The expression relating the vapor pressure of a metal to its relative ion current is

$$\ln P_i = \ln (K_R R_i^+ T).$$

Using equation I-2 to substitute for P_i one obtains

$$\ln (P_i^o a_i) = \ln (K_R R_i^+ T) \qquad \text{(II-16)}$$

The following relationships are provided from the expressions of Gibbs free energy for vaporization and the partial molar Gibbs free energy of mixing.

$$\ln P_i^o = - \frac{H_{VAP,i}^o}{RT} + \frac{S_{VAP,i}^o}{R} \qquad \text{(II-17)}$$

$$\ln a_i = \frac{H_i^M}{RT} - \frac{S_i^M}{R} \qquad \text{(II-18)}$$

From equations II-16, II-17, and II-18 the following expressions are determined.

$$\text{ALLOY} \quad \ln R_i^+ = \left(\frac{H_i^M - H_{VAP,i}^o}{R} \right) \left(\frac{1}{T} \right) - \ln T + K'$$

$$\text{PURE} \quad \ln R_i^+ = \left(\frac{-H_{VAP,i}^o}{R} \right) \left(\frac{1}{T} \right) - \ln T + K''$$

The difference of the above equations is the linear function with respect to 1/T of the logarithm of the normalized relative ion current used for the least squares curve fitting

$$\ln R_i^N = \frac{H_i^M}{R} \left(\frac{1}{T} \right) + K \, .$$

III. LITERATURE SURVEY

The following is a literature review of the previous investigations of the liquid metallic systems studied.

Cu-In

Activities were determined by galvanic cell measurements for a single temperature by Jagannathan and Ghosh[24] (1073°K, X_{In} = 0.2 - 0.8). The selected activity values of Hultgren, Orr, Anderson, and Kelly[25] are taken from the EMF study of Azakami and Yazawa[26] (1073°K, X_{In} = 0.2 - 0.8). These values and those of (2) are in good agreement showing a maximum discrepancy of 300 J at X_{In} = 0.7.

Kleppa's [27] calometric determination of the intergral molar heats of mixing (723°K, X_{In} = 0.978 - 0.921) are in fair agreement with those of Yazawa and Itagaki[28] (1373°K, X_{In} = 0.1 - 0.9) which are the basis of the selected values for Hultgren and Desai[29].

Cu-Ga

The activities and intergral molar heats of mixing were measured by Alcock, Sridhar, and Svedberg[30] (1550°K, X_{Ga} = 0.050 - 0.950). This mass spectrometric study was performed using the ion current ratio technique.

Cu-Si

Bowles, Ramstad, and Richardson[31] measured the activity of Si for low concentrations of Si by gas equilibrium (1833°K, X_{Si} = 0.051 - 0.0035)

Sn-Si

The literature search failed to provide any previous information on this system.

IV. TECHNIQUE EVALUATION

The sensitivity of the errors inherent to the relative ion current technique is estimated for a variety of experimental parameters using a hypothetical system. A test of the validity of these estimations is provided through a comparison of activities determined by this method and those in the literature.

Sensitivity Analysis

An evaluation of the error of a quantity determined from independently measured variables[32] is given by

$$\Delta Y = \left[\sum_{i=1}^{n} \left[\frac{d Y}{d X_i} \right]^2 (\Delta X_i)^2 \right]^{\frac{1}{2}} \qquad \text{(IV-1)}$$

where

ΔY = error of the determined quantity

X_i = the independently measured variable

ΔX_i = the small and randomly distributed absolute uncertainty of the measurement of the variable i

$\frac{dY}{dX_i}$ = the partial derivative of Y with respect to X_i

This method of analysis is used for the evaluation of the sensitivity of the relative ion current determinations of

activities and partial heats of mixing for a hypothetical study using variations in temperature and intensity uncertainties, number of data points per alloy, temperature interval, and magnitudes of activity and partial molar heat of mixing. The partials of equation II-15 are used in the calculations for activity. The least squares solution for the slope of a linear function is used in the evaluation for the partial molar heats of mixing.

Uncertainty in the ion intensity measurement is the major contributor to error in activity determinations. Using uncertainties of approximately twice that determined for the experimental work produces an activity error of eight percent. Doubling or tripling of the other parameters results in an error 1% or less.

The magnitude of the error of the partial molar heats of mixing determinations were found to be sensitive to all of the afore stated parameters except the magnitudes of the activity and partial molar heats of mixing. Applying values in equation IV-1 similar to those observed during the experimental study resulted in an estimated error of 4 kJ/mole. In order to reduce this error to less than 2 kJ/mole it is necessary to use twice the temperature interval and triple the number of ion intensity measurements as performed in this work. Both of these actions would increase the composition change of the sample through preferential volitalization of one of the alloy components. Furthermore, the temperature range is

limited by: (1) liquidus temperature, (2) machine sensitivity, (3) application of Kopp-Neumann rule, and (4) molecular/hydrodynamic flow transition.

The conclusion of this analysis is that the percent error in the activity measurements is less than 5% while the error of partial molar heats is of the order of 4 kJ.

The resolution of the apparent discrepancy in the differences in precision obtained for the two calculated quantities is demonstrated for a hypothetical case in figure 3. The minimum confidence interval for the fitted line is found at the center of the line, approximately the point where values for the activity are taken. The divergence of the confidence intervals from the fitted line at both ends of the line permits the construction of a second line within the interval. The difference of the slopes of this line from that of the fitted line corresponds to the error of the partial molar heat.

Comparitive Study

As a means of evaluating the actual application of the relative ion current technique selected alloys of the liquid Ag-Pb and Cu-Sn systems were studied.

Ag-Pb . The results from the galvanic cell investigation of this system by Hager and Wilkomirsky[33] show excellent agreement with the literature values compiled by Hultgren, Orr, Anderson, and Kelly[25]. The normalized relative ion currents of

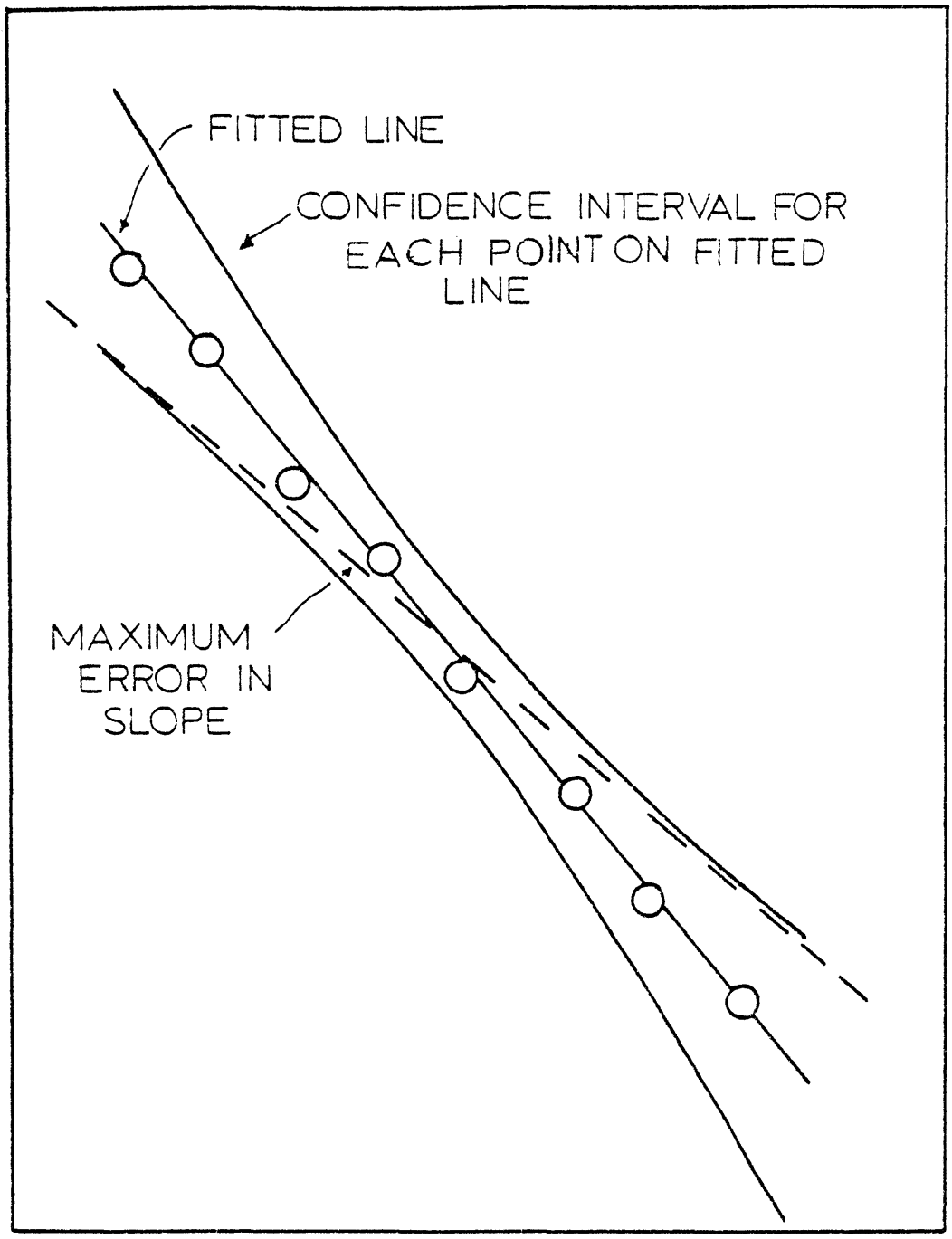

FIG. 3 - HYPOTHETICAL PLOT OF CONFIDENCE INTERVAL FOR A LINEAR FUNCTION.

lead for selected alloy compositions were measured, figure 4, and the calculated activities compared to those given by (33), Table I. The standard chosen was the previously studied Pb-Au alloy[34] of $X_{Pb} = 0.188$.

$$a_{Pb}^{STD} = 0.084$$

This study demonstrates the error in activity measurements by this technique is within the estimated 3 percent. The excellent reproducibility of these measurements is indicated on figure 4 by the duplicate studies of the alloy at $X_{Pb} = 0.103$.

Cu-Sn. The normalized relative ion currents of Cu and Sn for various compositions are shown in figure 5. The standards were chosen as the pure metal for both components.

$$a_{Cu}^{STD} = a_{Sn}^{STD} = 1$$

The activities determined by this method are shown in Table II. Also shown on Table II are the values measured using ion current ratio technique[35] which are in good agreement with other literature values[25]. The comparison of the tabulated values again demonstrate the precision of this Knudsen cell - mass spectrometer method.

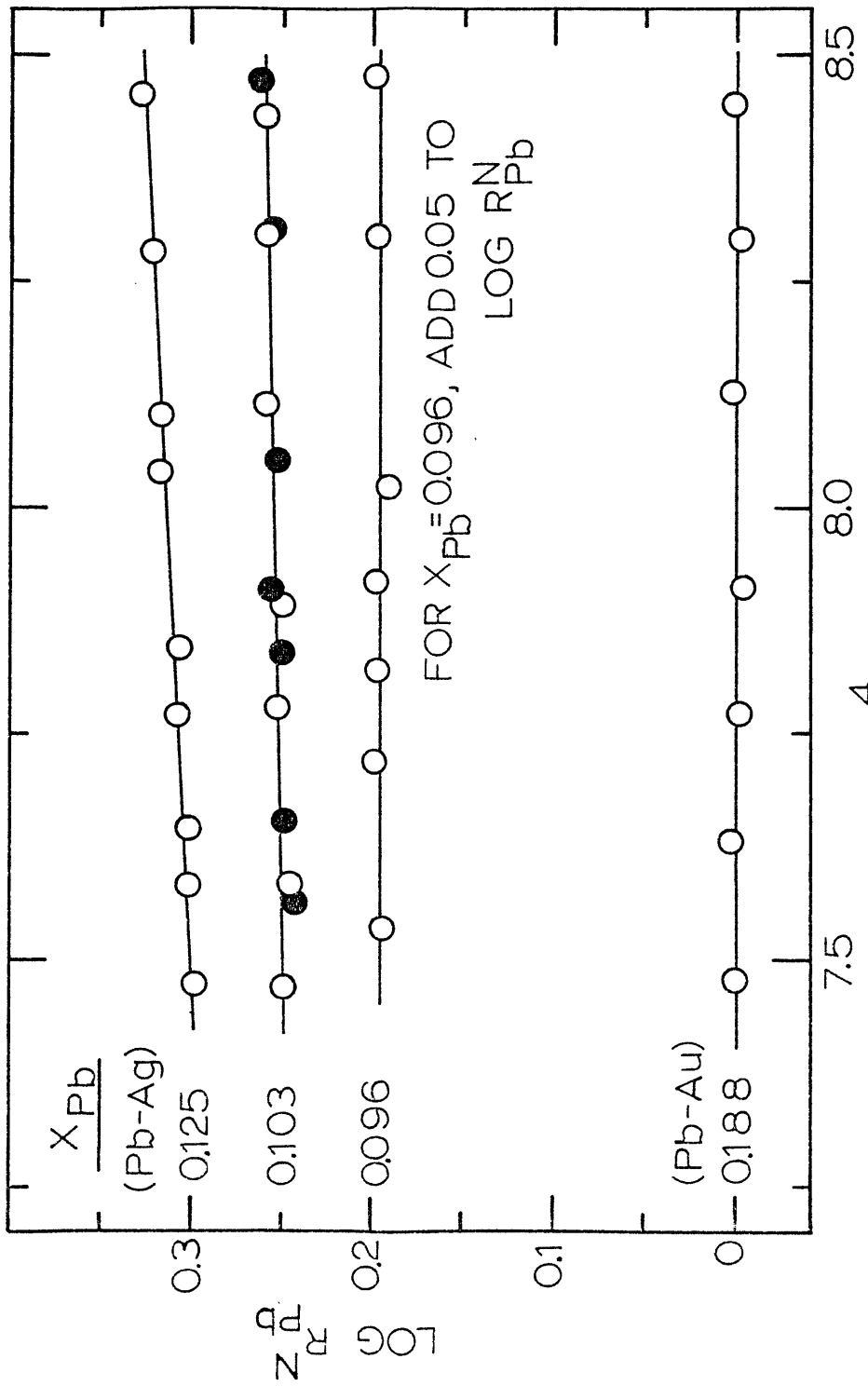

FIG. 4 - NORMALIZED RELATIVE ION CURRENTS OF Pb FOR SELECTED COMPOSITIONS OF THE LIQUID Ag-Pb AND Au-Pb SYSTEMS.

TABLE I

COMPARISON OF ACTIVITIES OF Pb FOR

LIQUID Pb-Ag SYSTEM AT 1200^{O}K

X_{Pb}	THIS STUDY (±0.008)	PREVIOUS STUDY (40) (±0.006)	DEVIATION
0.125	0.176	0.181	2.8%
0.103	0.152	0.154	1.3%
0.096	0.146	0.143	2.0%

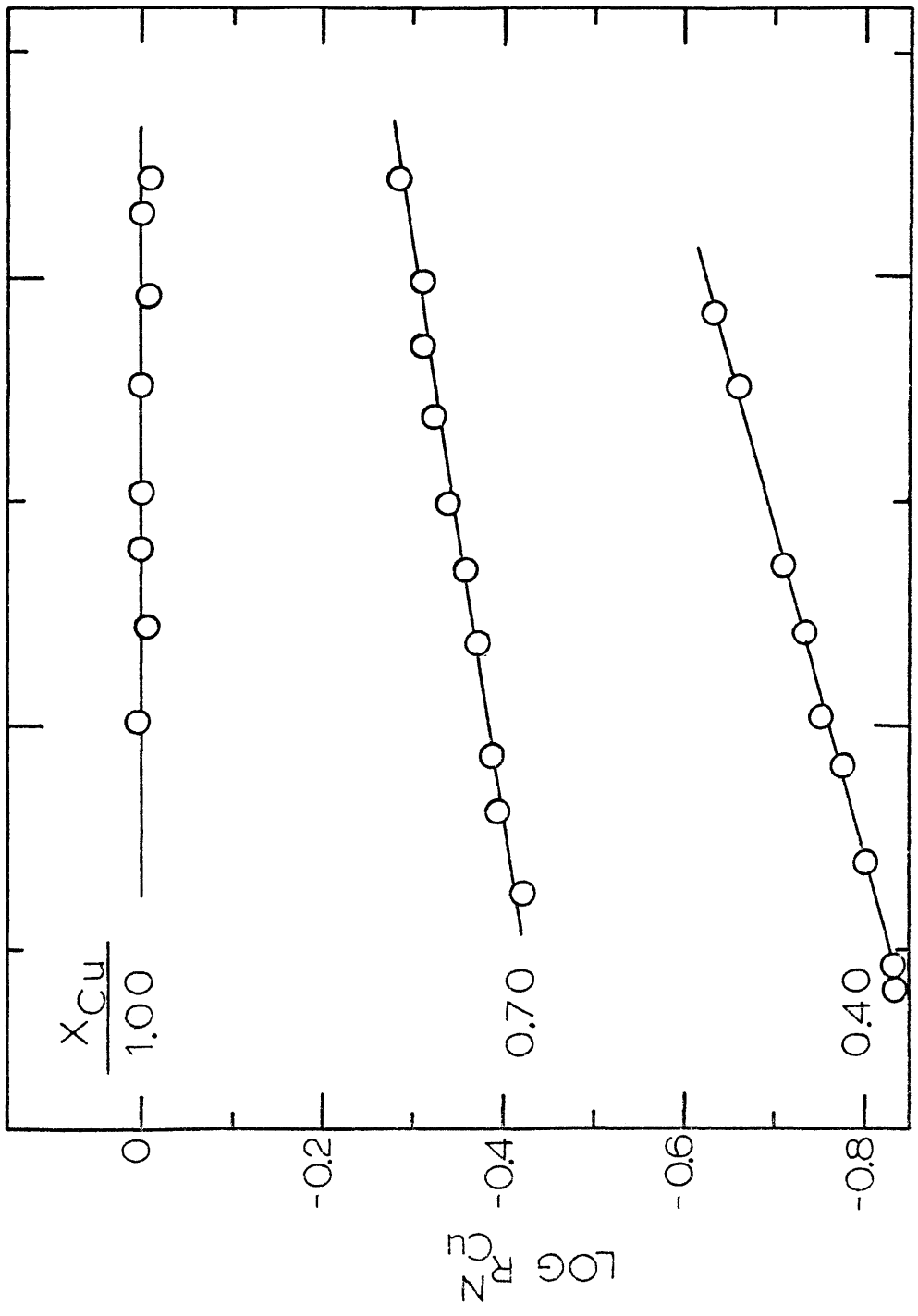

FIG 5.a- NORMALIZED RELATIVE ION CURRENTS OF Cu IN THE LIQUID Cu-Sn SYSTEM.

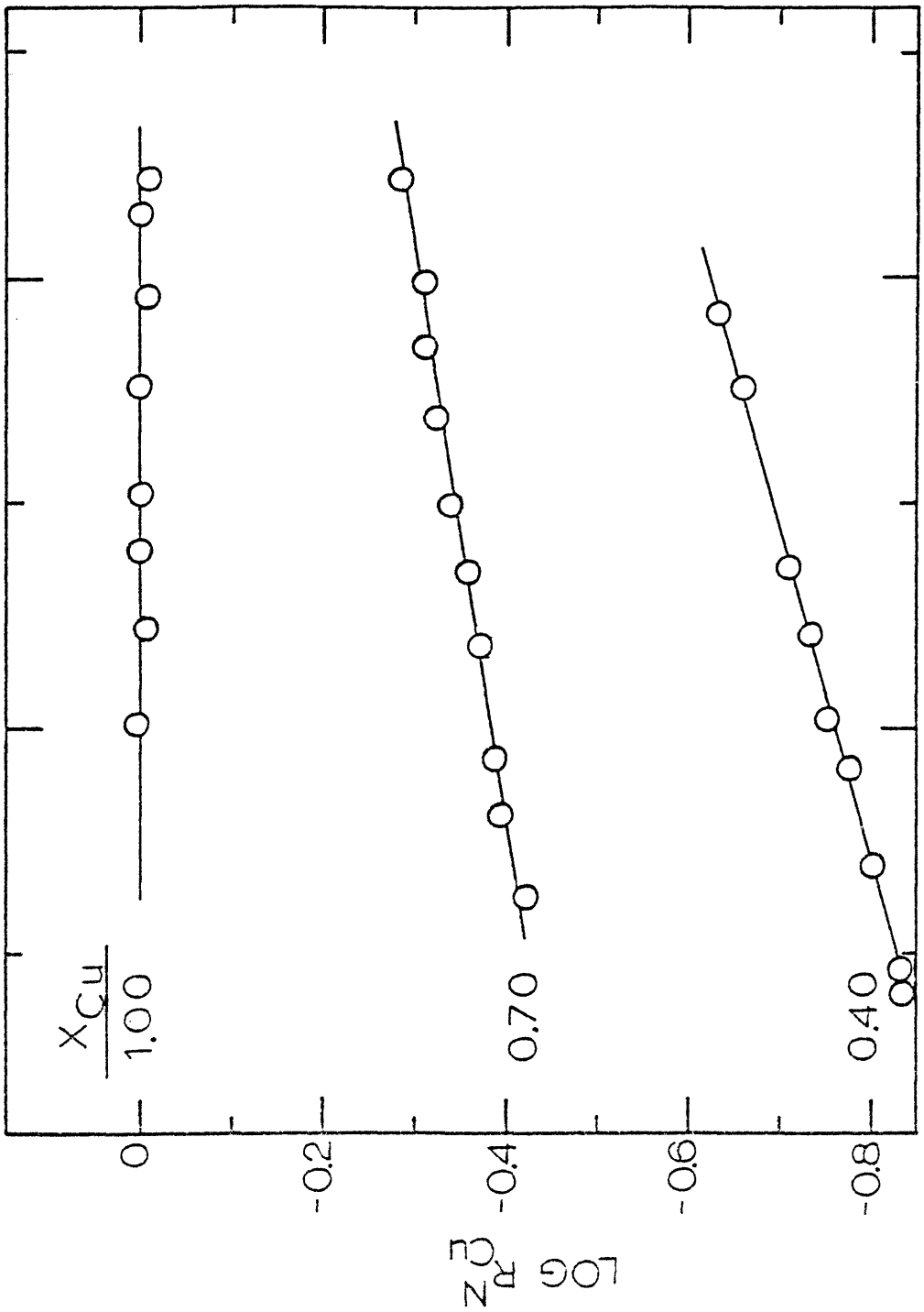

FIG 5.a- NORMALIZED RELATIVE ION CURRENTS OF Cu IN THE LIQUID Cu-Sn SYSTEM.

TABLE II

COMPARISON OF ACTIVITIES FOR

THE Cu-Sn SYSTEM AT 1573°K

	(THIS STUDY)	(PREVIOUS STUDIES) (42)		(THIS STUDY)	(PREVIOUS STUDIES) (42)	
X_{Sn}	a_{Cu}	a_{Cu}	DEVIATION	a_{Sn}	a_{Sn}	DEVIATION
0.30	0.463(±0.004)	0.472(±0.006)	-1.9%	0.193(±0.004)	0.201(±0.002)	-4.0%
0.60	0.215(±0.004)	0.210(±0.003)	+2.4%	0.571(±0.004)	0.577(±0.001)	-1.0%

V. EQUIPMENT AND PROCEDURE

Mass Spectrometer

A Bendix model 12-101A Time of Flight Mass Spectrometer was used for the initial phases of this work. This system's electronics were updated to solid state components by the installation of a modified CVC-MARK-4 Retrofit unit, figure 6. The benefits of the above modification are an increase in the stability of the pulses and voltages, and a decrease in the electronic background noise. A comparison of the results obtained from the two systems indicated a significant increase in the precision of the ion intensity measurements by the new electronics. Both instruments perform ten thousand mass analyses per second with a maximum resolvable mass of approximately 700 atomic mass units. As detailed discussions of the theory of operation have been previously given [36,37] only a brief description of a single cycle is given in the following.

The vapors or molecular beam effusing from the Knudsen cell enter the mass spectrometer after passing through a series of collimating slits seen on figure 7. The molecular beam then enters ionization regions of the ion source where ions are formed by electron impact. The energy and number of electrons in the electron beam are separately controlled. The

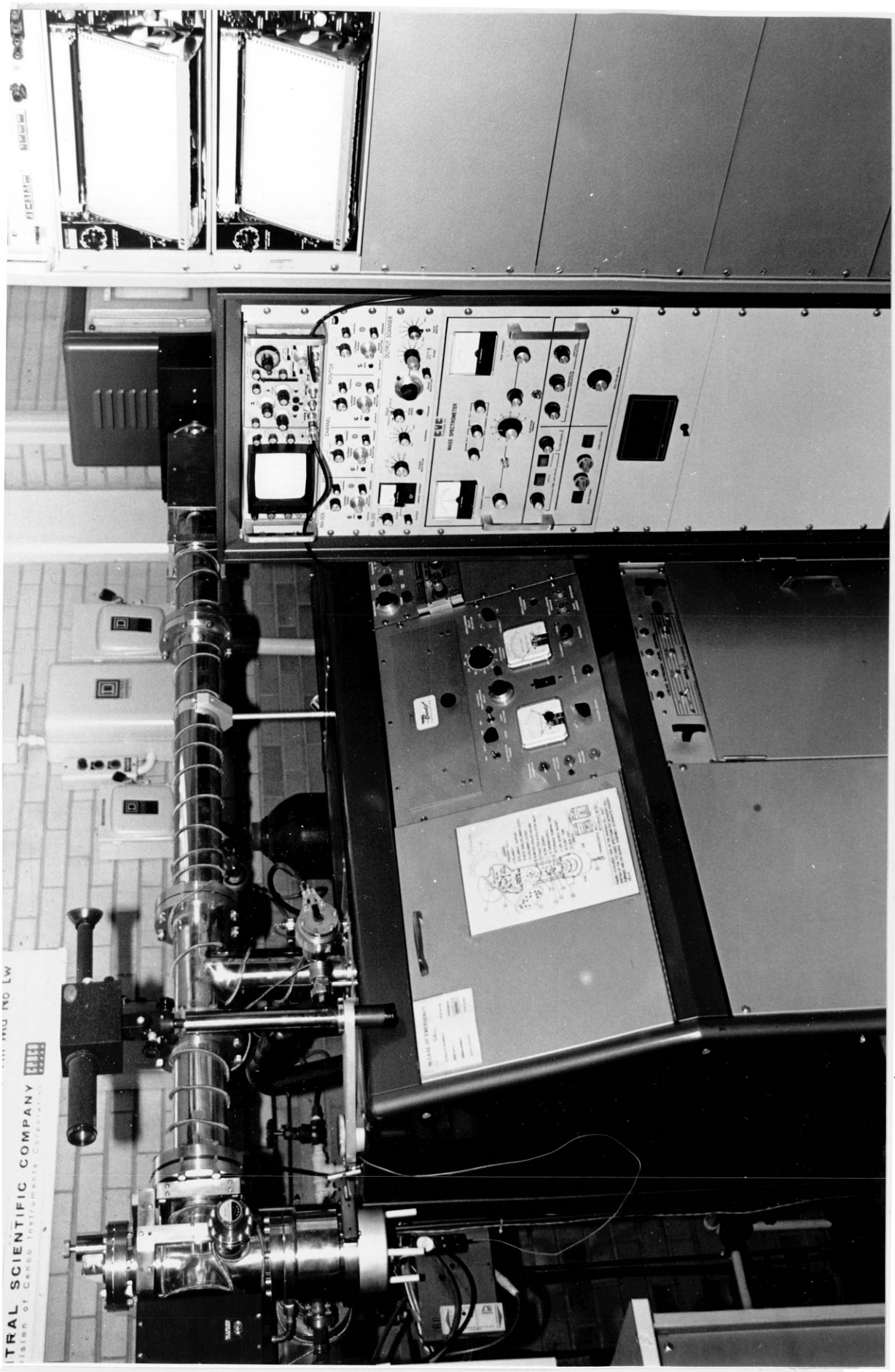

Figure 6. Overall View of the Time-of-Flight Mass Spectrometer.

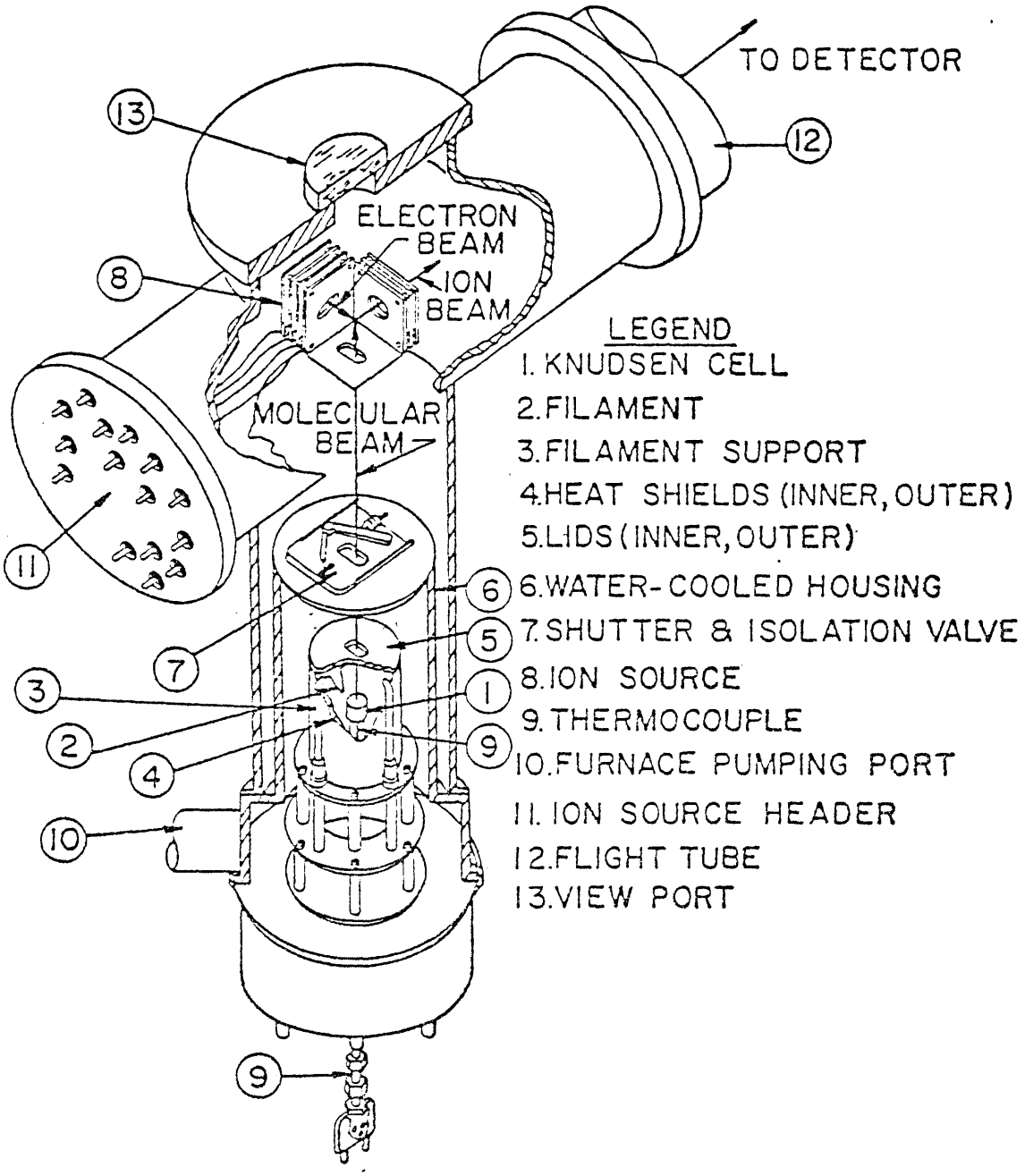

FIG. 7 - CUT-AWAY VIEW OF THE KNUDSEN CELL INLET SYSTEM OF THE T.O.F. MASS SPECTROMETER.

flow of ionizing electrons, the electron beam, is stopped and a negative potential is applied to the ion drawout grid. The positively charged ions removed from the ionization region by this potential are further accelerated into the flight tube by a series of high voltage ion acceleration grids. As the ions traverse the flight tube they separate into groups having equivalent mass to charge ratios. This separation is seen by the relation of the kinetic energy produced by the ion acceleration grids to the velocities of the ions.

$$q_i E = \tfrac{1}{2} M_i V_i^2$$

where

q_i = charge of ion i

E = potential drop through ion grids

M_i = mass of ion

V_i = velocity of ion.

The time for an ion to traverse the flight tube of length l, the time of flight, t, is

$$t = l\,(2q_i E/M_i)^{-\frac{1}{2}} = \text{constant} * (M_i/q_i)^{\frac{1}{2}}$$

It can be seen from this equation that ions of different M/q ratios require different times of flight. Therefore, a packet of ions of a specific M/q ratio reaches the detector at a unique time. The ions in these packets impact the detector

and produce secondary electrons. These electrons are amplified to a measurable current by the magnetic electron multiplier. This current is called the ion current and denoted by I_i^+.

A mass spectrum of the initial molecular beam is produced by plotting these currents against their corresponding time of flight. A second form of the output is the constant measurement of the ion current of a particular M/q ratio by the analog scanner.

Knudsen Cell Inlet

The Bendix Knudsen cell inlet assembly and furnace controller are shown in figures 6 and 7. The Knudsen cell is supported by three tungsten rods. Two of the rods are stationary while the third is adjustable from the exterior of the housing to allow positioning of the cell under vacuum. The cell is surrounded by a series of tantalum heat shields. The lids of the heat shields are slitted to allow passage of the molecular beam. The shutter-isolation valve assemblage is located above these lids. This assemblage has three positions. The first position isolates the Knudsen cell inlet from the ion source by a vacuum seal. The second position permits the molecular beam to enter the ion source. The third position places a cold stainless steel plate between the Knudsen cell and the ion source. The stainless plate condenses any high temperature vapors produced by the Knudsen cell allowing

background determinations.

The Knudsen cell is heated by two U shaped tungsten filaments. The furnace control has two distinct modes of heating: radiation and bombardment. In the radiation mode, the cell temperature is controlled between 0 and 1100°K by varying the current passing through the filaments. Cell temperatures from 900 to 2500°K are attained in the bombardment mode by electron impact on the cell. The electron impact effect is produced when a -1200 volt potential is applied to the filament while maintaining the cell to ground. The number of electrons which strike the cell (i.e. the temperature of the cell) is controlled by varying the current through the filaments. The thermocouple used for temperature determination extends through an O-ring seal at the tower base plate into the center of the Knudsen cell.

Knudsen Cell

The two styles of Knudsen cells used throughout this study are drawn in figure 8. The design utilizing a boron nitride liner was used exclusively for the silicon alloy system. All cells used were 3 cm in height with an outside diameter of 1.6 cm. The approximate orifice diameters of the sample and reference chambers was 0.38 mm and 0.26 mm, respectively. Materials used in cell construction are AFX grade POCO graphite and National boron nitride.

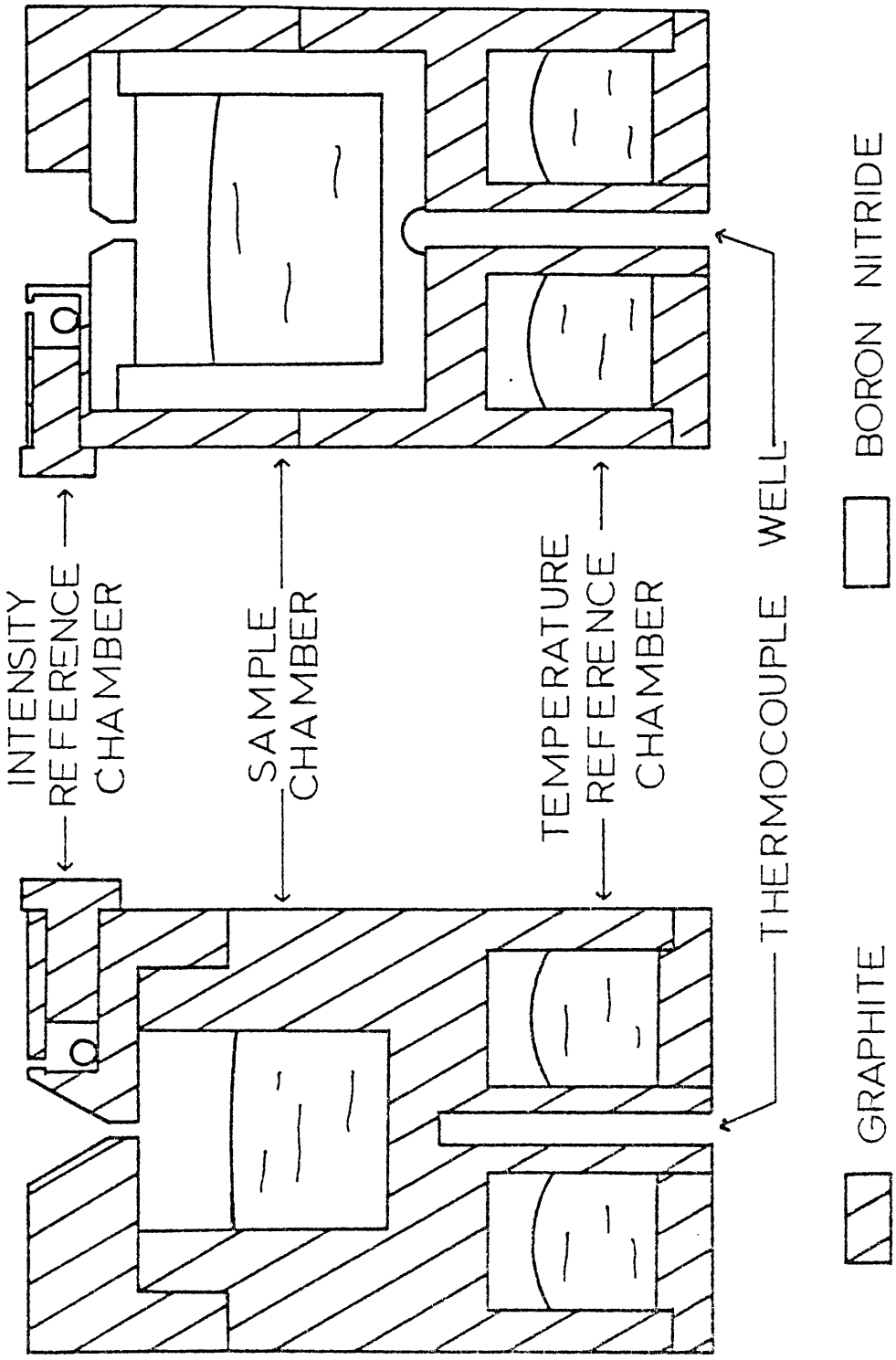

FIG 8- KNUDSEN CELLS USED FOR RELATIVE ION CURRENT MEASUREMENTS

Sample Preparation

All metals used in sample preparation have purities of 99.99% or greater. Samples are prepared from weighed amounts of pure metal and fused in the Knudsen cell. Comparisons by this author and previous investigators[2] of the results obtained when samples are premelted and when they are fused in the Knudsen cell have shown that premelting is not necessary if a heat up procedure is followed as outlined in the following sections.

Temperature Measurement

Temperature of the cell is measured by a 1/16 in., tantalum sheathed, grounded junction, W5%Re - W26%Re thermocouple. An Omega cold-junction compensator is used to fix the reference junction temperature. The EMF of the thermocouple is measured to the nearest 0.02 mv. by a Leeds and Northrop Speedomax W-AZAR recorder and/or a Hewlett-Packard Differential Volt meter. Each thermocouple is calibrated by measuring the EMF corresponding to the melting of pure metals in the Knudsen cell. The metals used are Ag, Au, Cu, Ni, and Fe. The melting points of these metals are determined by three methods. The melting points of Cu, Ni, and Fe are determined visually through the use of an optical pyrometer which is used to sight into the cell through the orifice. Thermocouple arrests are obtained for Ag, Au, and Cu and ion intensity arrests are measured for Ag. Excellent agreement

is found between all three methods.

Corrective shifts of the thermocouple calibration curve are determined for each experiment by the thermal arrest produced by the fusion of the temperature reference metal. These shifts are due to variations of thermocouple positioning in the thermocouple well and do not affect the calibration of the thermocouple. The corrective shifts encountered in the cells used are of the order of 2 to 5°K.

General Procedure

The pure materials are weighed and then sealed in the sample chamber by the Knudsen cell lid. A small bead of Zn is placed in the reference chamber which is then sealed by a graphite plug. The cell is positioned in the tower and the heat shield lids are put in place. The alignment of the reference and sample orifices is checked by adjusting the position of the cell by the exterior control so that one orifice and then the other appears directly below the heat shield lid slit. If these orifices do not exactly replace one another, the cell is removed and its lid rotated. The cell is repositioned in the tower and alignment checked. This process is repeated until orifice alignment is judged satisfactory.

The tower is now placed into the inlet and the system is evacuated to 1 to 10 nanopascals.

The electronic parameters are set and the system is allowed to stablize for at least 10 minutes. After this time the furnace is powered and the reference orifice is optically

positioned beneath the ion source. The analog scanner is set to the 64 amu. isotope of Zn and the ion current is maximized by adjustment of the cell position, and ion optics. The reference intensity is then measured. The length of the reference intensity arrest is normally of the order of 2 to 3 minutes. This intensity is taken as the difference of the analog output with the shutter open and closed. After the zinc has completely vaporized at a temperature of approximately 700^{o}C, the cell is repositioned with the sample orifice beneath the ion source. The temperature is raised and the thermal arrest of the reference metal is determined as it melts. The cell is now heated to the maximum analysis temperature and the analog scanner is set to the ratio of the largest isotope of the species of interest. The ion current is again maximized by cell position and ion optics adjustments. After several minutes have past to allow homogenization of the sample, the temperature and ion intensity are recorded. This ion intensity is the difference of the analog output with the shutter open and closed. The temperature is then lowered by 20 to 30^{o}C. Temperature and ion intensities are again measured after thermal equilibrium is established. In a similar manner, ion intensity and temperature measurements are made for the remainder of the temperature range of interest.

After the measurements are completed the furnace is cooled and the sample weighed. The loss of sample weight is

used to determine the maximum composition change possible.

The relative ion currents are now calculated by dividing each ion intensity measured by the reference intensity. The logarithm of the relative currents values are then used in conjunction with the equation for the standard relative ion current to calculate the normalized values. A linear function equation I-16 is fit to this normalized data by least-square regression analysis. The activity and partial molar heat of mixing is taken from this equation. The activities and partial molar heats of mixing are determined for the second alloy component after the first component has been defined over the entire composition range. These quantities for the second component are calculated through the application of the alpha and beta functions [6,15], Appendix I. Due to the large degree of scattering of the partial molar heats and the sensitivity of the beta function to such scatter, a smooth curve is drawn through the measured quantities and values are taken from this curve to calculate the beta function.

VI. ERROR ANALYSIS

The analysis and elimination of the systematic errors associated with the relative ion current technique is examined in this chapter. The sources of systematic error discussed are temperature measurement, composition variation, diffusion, effusion, and molecular and polymer species. The procedure used in the error analysis of the experimental data is also presented.

Systematic Errors

Temperature Measurement. To insure accurate temperature measurements, three procedures are followed. First, each thermocouple is calibrated for the cell design and material as outlined in chapter V. The second precaution taken, also described in chapter V, is the temperature reference determinations performed for each experiment to account for positioning of the thermocouple in the thermocouple well.

A demonstration of this positional calibration is shown for a hypothetical experiment in figure 9. The reference melting point r for the test is determined to be lower than that predicted by the calibration curve. The calibration curve is shifted down to agree with the reference value. This

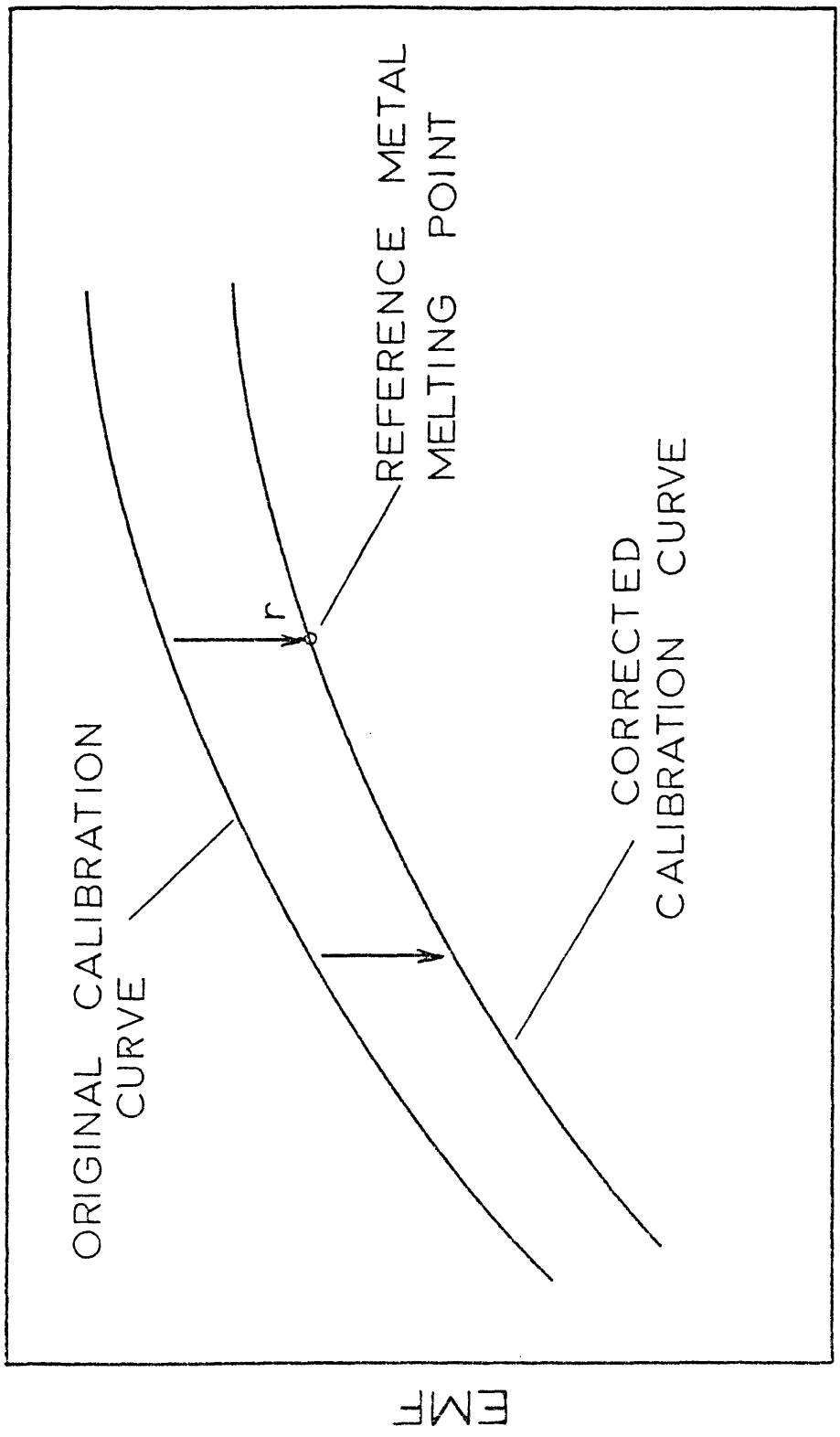

FIG. 9——HYPOTHETICAL CORRECTION FOR THERMOCOUPLE POSITIONING

corrected curve is then used for temperature measurements throughout the run. It has been found through experimental melting point determinations that this correction does not affect the original calibration curve and thus contributes no error in temperature measurement.

The third procedure followed is the evaluation of the thermal gradient of the cell by a series of experiments. These experiments consist of the comparisons of the melting points of Ag, Au, and Cu at various positions in the cell. The thermal gradient of the cell as determined by this method is of the order of $1^{o}K$ or less for the graphite cell and $4^{o}K$ or less for the cell using boron nitride.

Further verification of the temperature measurement system is provided by the excellent agreement of the heats of vaporization measured by this system and the literature values. The equation used for these determinations is developed in Appendix II.

$$\frac{d \ln (R_i^+ T)}{d (1/T)} = - \frac{H^o_{VAP,i}}{R}$$

The results from these measurements are given on table III. The uncertainty in the temperature indicated by these measurements, neglecting any error in the ion intensity values, is of the order of 5 to $10^{o}K$.

The overall errors in temperature measurement for the graphite cells and cells using boron nitride are ± 2 and ± $5^{o}K$,

TABLE III

COMPARISONS OF HEATS OF VAPORIZATION FOR PURE METALS

	EXPERIMENTAL kJ/mole	LITERATURE (26) kJ/mole	DEVIATION kJ/mole	TEMPERATURE ^{o}K
Ag	262.9	264.1	1.2	1325
Cu	321.9	314.5	7.4	1500
Ga	266.1	263.6	2.5	1500
In	232.1	234.4	2.3	1473
Sn	292.3	296.4	4.1	1723

respectively.

Sample Composition. Several experimental sources may account for sample composition changes. These sources are contamination, depletion, and nonhomogeneous mixing.

Contamination of the sample can be caused by diffusion of the intensity or temperature reference metals through the walls of the sample chamber. Both of these modes of contamination are neglected as no detectable accumulation of either metal is found in pure silver after repeated runs. The possibility of contamination from the temperature reference chamber is further reduced by selecting pure Cu as the reference metal which is a component in all but one of the alloy systems studied.

Nonhomogeneous mixing of the sample would be characterized by a gradual change of the ion intensity at constant temperature. As this phenomenon has never been observed and as premelting has shown no effect on the relative ion intensity measurements, the samples are assumed to be homogenized by the heat up procedure outlined in chapter V.

Bulk depletion of a component of a sample is a major consideration in composition variation. Bulk depletion occurs when there are large differences in the effusion rates (i.e. the partial pressures) of the components. This action is equivalent to fractional distillation. Three measures are taken to minimize this fractionation: (1) maximizing sample

weights, (2) minimizing time spent at high temperatures, and (3) minimizing the sample orifice diameter. Weight losses of each sample are used to calculate maximum composition changes. These calculated changes are one percent or less for the systems studied.

Surface depletion occurs when the molar flux of an element from the bulk of the sample to the sample surface is less than the molar flux of the element through the orifice. The extent of surface depletion is dependent upon the ratio of the surface area of the sample to the area of the orifice. An increase in this ratio results in a decrease in the extent of the depletion. A variety of values for this ratio were used in measuring normalized relative intensities for selected compositions. The results of these measurements are consistent with experimental error. The error due to surface depletion is, therefore, considered negligible.

Diffusion. There are two forms of diffusion which may contribute to the effusing molecular beam, surface and bulk.

Surface Diffusion - The Knudsen effusion equation II-1 is derived from the assumption that a gas species striking a site of the cell or orifice wall is reflected or re-evaporated from the same site. Investigations [38,39] have been demonstrated that in the vicinity of the orifice a significant amount of surface diffusion through the orifice can occur before re-evaporation, that is the site of evaporation is not the site of

adsorption. The ratio of molar fluxs from the surface diffusion-evaporation mechanism and Knudsen effusion is dependent upon the geometry of the orifice. This ratio approaches zero for conical orifices of the dimensions used in this study. This conclusion is verified by the excellent agreement obtained in the heat of vaporization studies. The effect of surface diffusion is therefore neglected.

Bulk Diffusion - The diffusion through the walls of the cell is termed the bulk diffusion. Of the elements studied, only copper has shown any significant bulk diffusion. The significance of this diffusion is measured by the comparison of the ion intensity for a component produced through a given orifice to that produced when there is no orifice. The contribution due to copper bulk diffusion was found to be reduced to an acceptable level, less than 3%, by increasing the lid thickness from 1/16 to 3/16 - in.

Effusion. The two possible types of effusion through a Knudsen cell orifice are molecular and hydrodynamic [18]. Molecular flow occurs when the ratio of the mean free path λ to the orifice diameter is greater than 10. As this ratio decreases, the flow proceeds through a transition region to complete hydrodynamic flow. An equation for the relative ion current in the hydrodynamic flow region can be derived in a similar manner as is shown in chapter III. This equation will differ from the equation for molecular flow in the values of

the constants. Thus the relative ion current technique is applicable to the hydrodynamic flow region.

The molar flux through the transition region is some complex function of both molecular and hydrodynamic flow. As this function must be dependent upon the total pressure of the sample (i.e. the sample composition), the normalized relative ion currents in equation I-15 becomes meaningless. To avoid this transition effect all relative ion current measurements are made in the molecular flow region.

Molecular and Polymer Species. Fragmentation of molecules and polymers by the ionizing electron beam can contribute to the lower mass ion currents. This effect can be ignored for polymers if the ion intensity measured is that of the polymer of the highest molecularity, Appendix III. For the case involving volatile compounds or large polymers of low pressure, the contribution due to dissociative ionization must be determined. This determination can be made by measuring the variation in the ion intensity with electron energy as described by Hager, Howard, and Jones [40].

All of the metals studied are reported to form dimers and/or higher order polymers[41,42]. These reported polymers all have vapor pressures of less than one percent of the monimer. Mass spectrums taken at high amplification for various compositions, temperatures, and electron energies indicated that no polymers or molecular species existed for any of the alloy

systems.

Data Analysis

A 90% confidence interval [43] was determined for both the activity at the temperature reported and the partial molar heat of mixing for each alloy studied. Of the systems studied this interval was less than 3% of the activity values. The partial molar heats analysis produced intervals of 4 to 8 kJ/mole.

VII. RESULTS

The results of the studies of the liquid binary alloys are presented in this chapter. The following plots are given for each alloy system: (1) normalized relative ion current, (2) activity and partial molar heats of mixing from R_i^N plots, (3) alpha and beta functions, and (4) summary of activity and integral molar heat of mixing. The final results for each system are tabulated at the end of each series of plots.

The 90 percent confidence interval for the activities is less than three percent of any activity value. The confidence intervals for the relative partial molar heats are of the order of 4 to 6 kJ/mole.

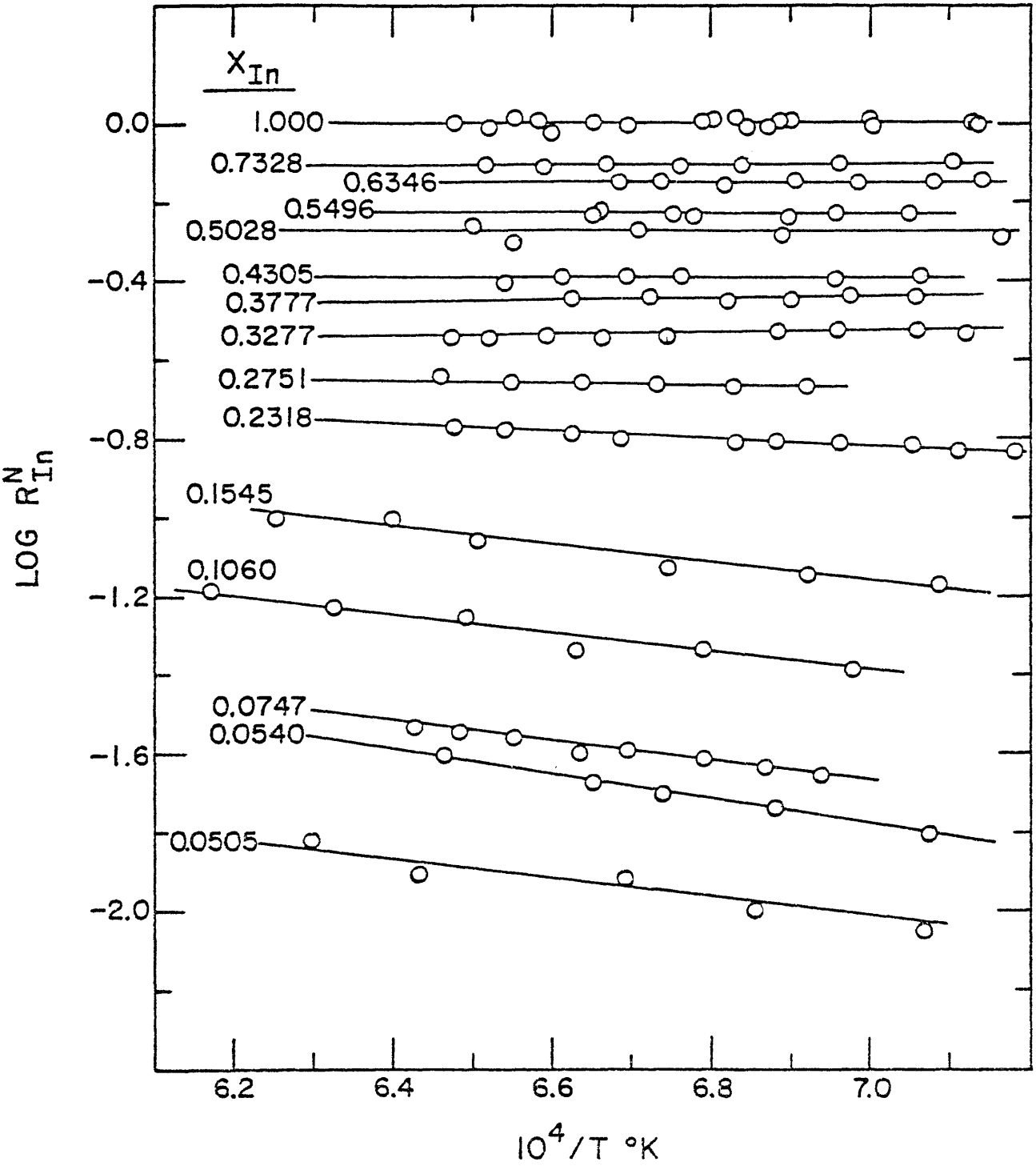

FIG. 10-NORMALIZED RELATIVE ION CURRENTS OF In FOR THE LIQUID Cu-In SYSTEM.

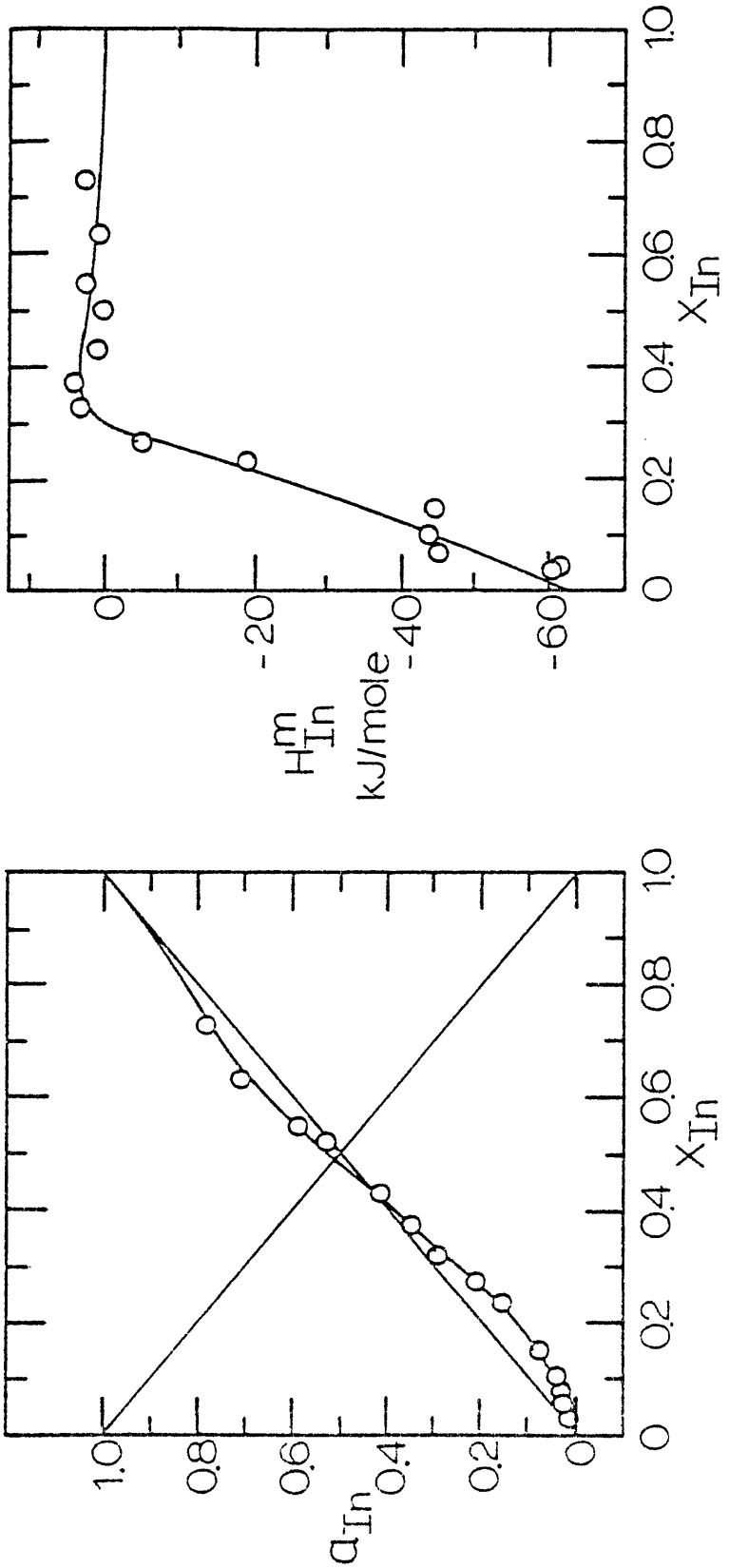

FIG. 11- RESULTS FROM THE NORMALIZED RELATIVE ION CURRENT PLOT FOR THE LIQUID Cu-In SYSTEM:(a) ACTIVITIES OF In AT 1473°K; (b) PARTIAL MOLAR HEATS OF MIXING OF In.

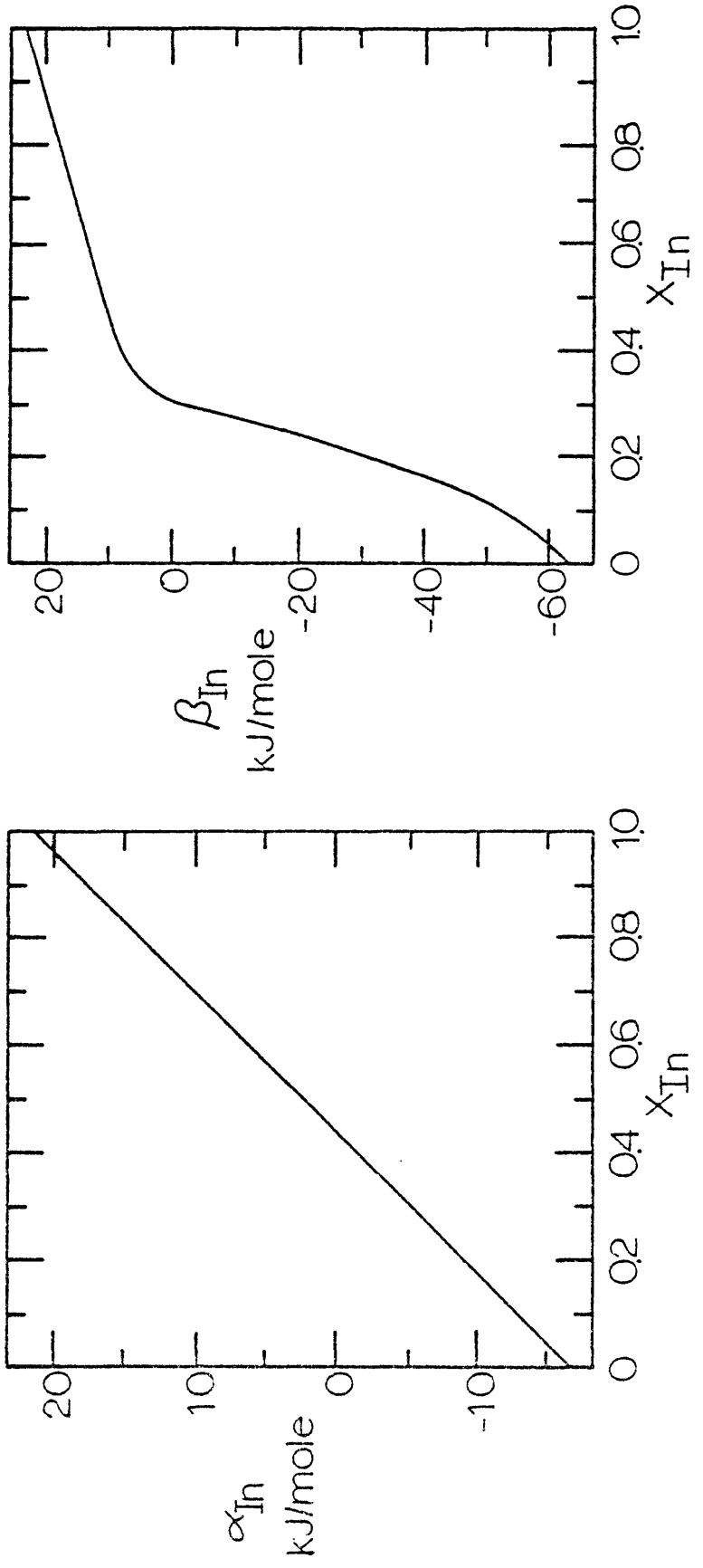

FIG. 12 - INTEGRATION PLOTS FOR THE LIQUID Cu-In SYSTEM AT 1473°K:
(a) In ALPHA FUNCTION; (b) In BETA FUNCTION.

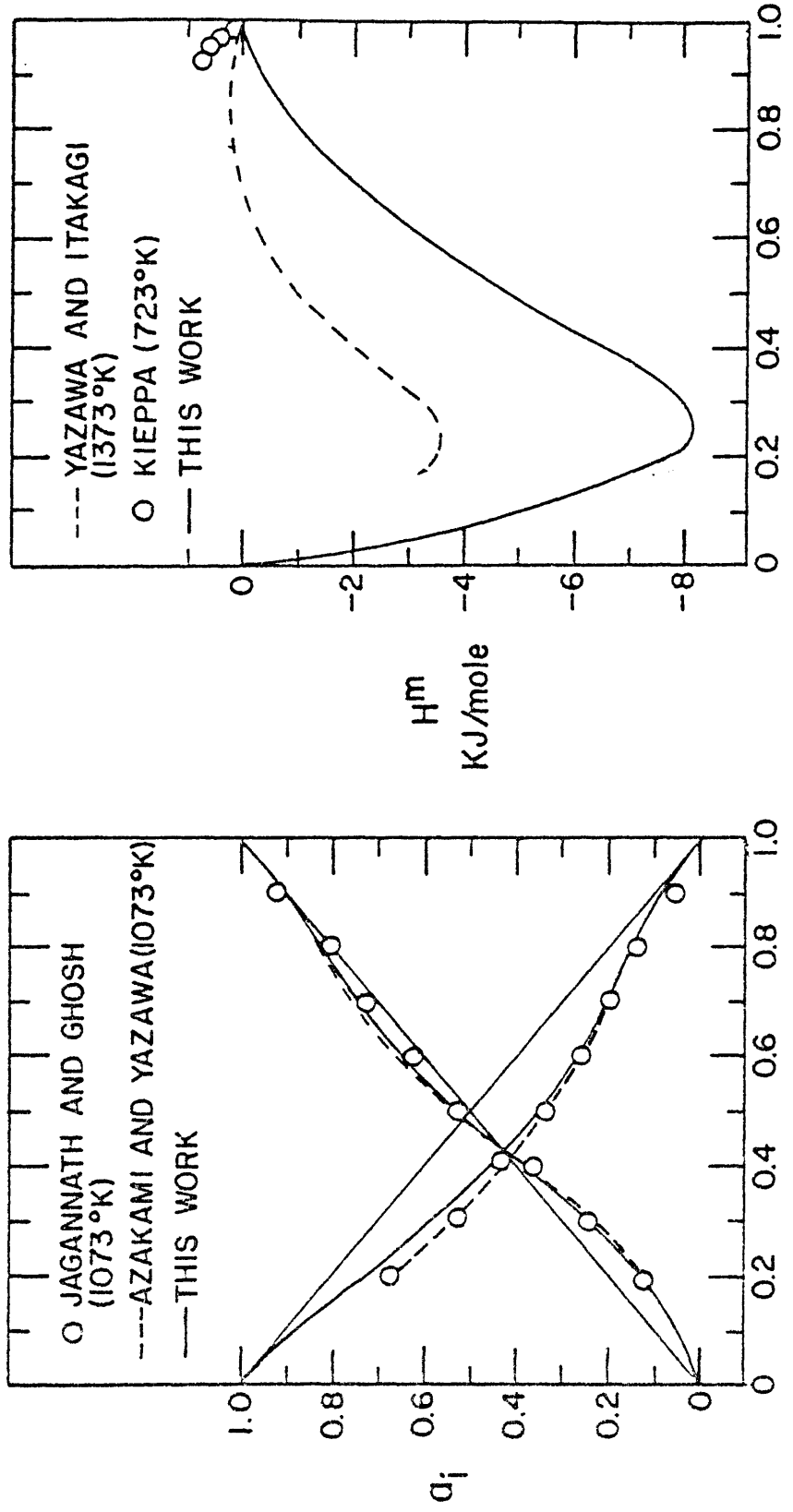

FIG. 13–SUMMARY OF RESULTS FOR THE LIQUID Cu–In SYSTEM AT 1473 °K: (a) ACTIVITIES; (b) INTEGRAL MOLAR HEAT OF MIXING.

TABLE IV

RESULTS FOR THE LIQUID Cu-In SYSTEM AT 1473°K

X_{In}	a_{In}	γ_{In}	a_{Cu}	γ_{Cu}	H_{In}^{M} kJ/mole	H_{Cu}^{M} kJ/mole
1.00	1.000	1.000	-	1.196	0	-1.02
0.90	0.913	1.014	0.0898	0.898	0.21	-5.12
0.80	0.836	1.045	0.150	0.750	0.42	-8.11
0.70	0.756	1.080	0.207	0.690	1.46	-10.34
0.60	0.649	1.082	0.272	0.680	2.09	-11.53
0.50	0.523 (±0.016)	1.042 (±0.027)	0.354 (±0.011)	0.708 (±0.021)	2.51 (±6)	-12.06 (±6)
0.40	0.381	0.953	0.457	0.762	3.35	-12.74
0.30	0.241	0.803	0.584	0.834	0.00	-11.44
0.20	0.123	0.615	0.729	0.911	-20.08	-4.85
0.10	0.0421	0.421	0.877	0.974	-41.84	-1.07
0.00	-	0.251	1.000	1.000	-62.76	0

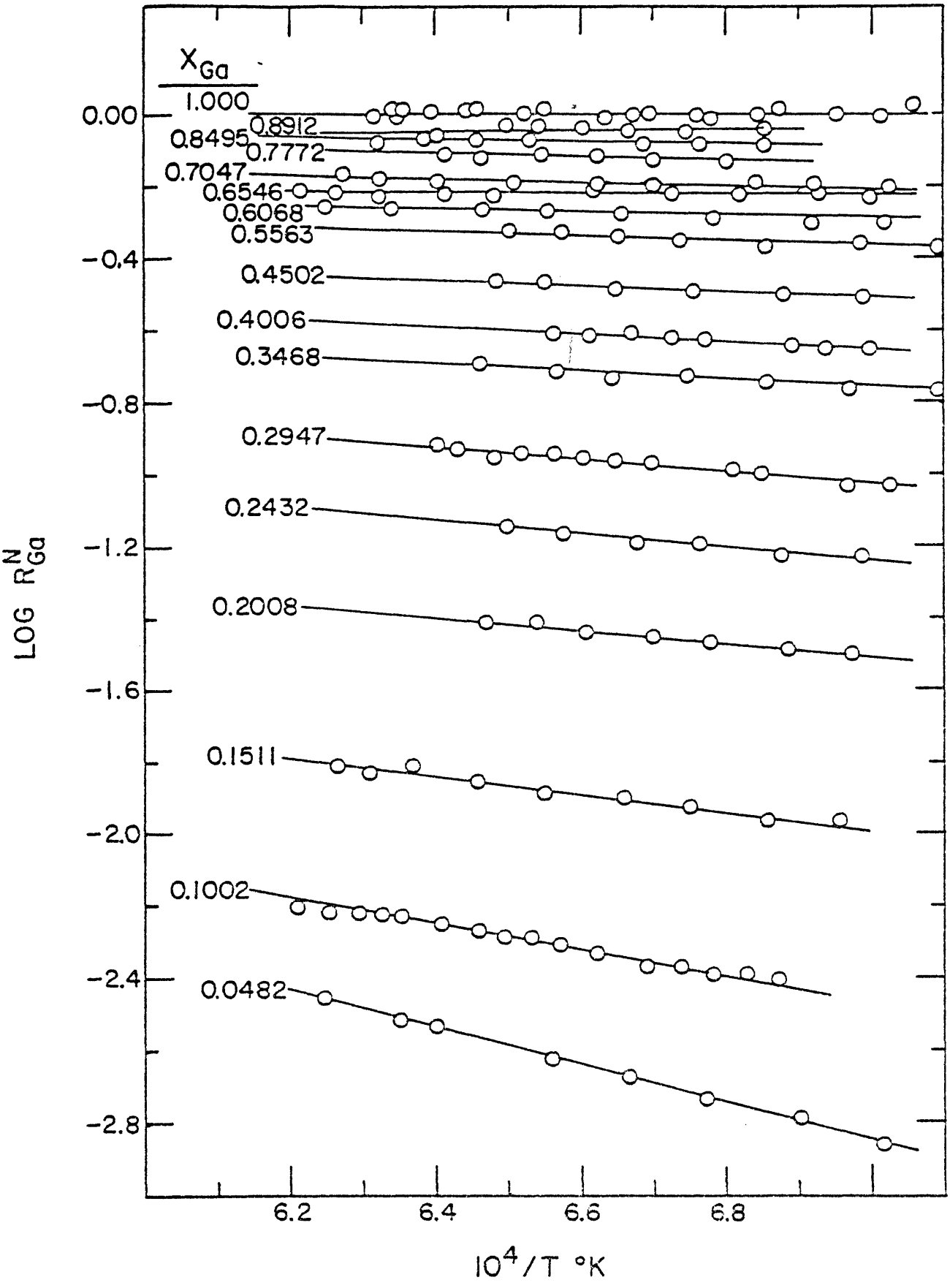

FIG. 14-NORMALIZED RELATIVE ION CURRENTS OF Ga FOR THE LIQUID Cu-Ga SYSTEM.

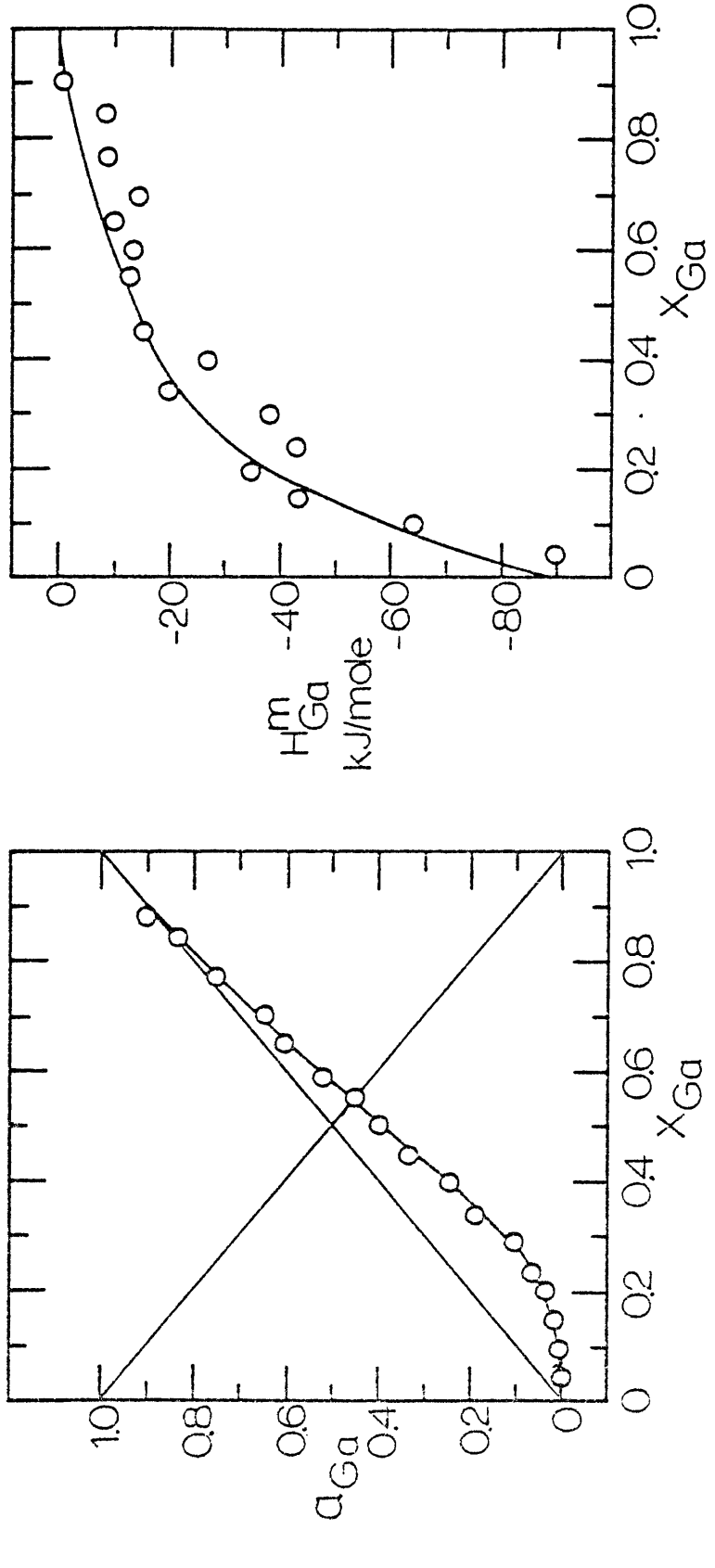

FIG. 15 - RESULTS FROM THE NORMALIZED RELATIVE ION CURRENT PLOT FOR THE LIQUID Cu-Ga SYSTEM:(a) ACTIVITIES OF Ga AT 1500°K; (b) PARTIAL MOLAR HEATS OF MIXING OF Ga.

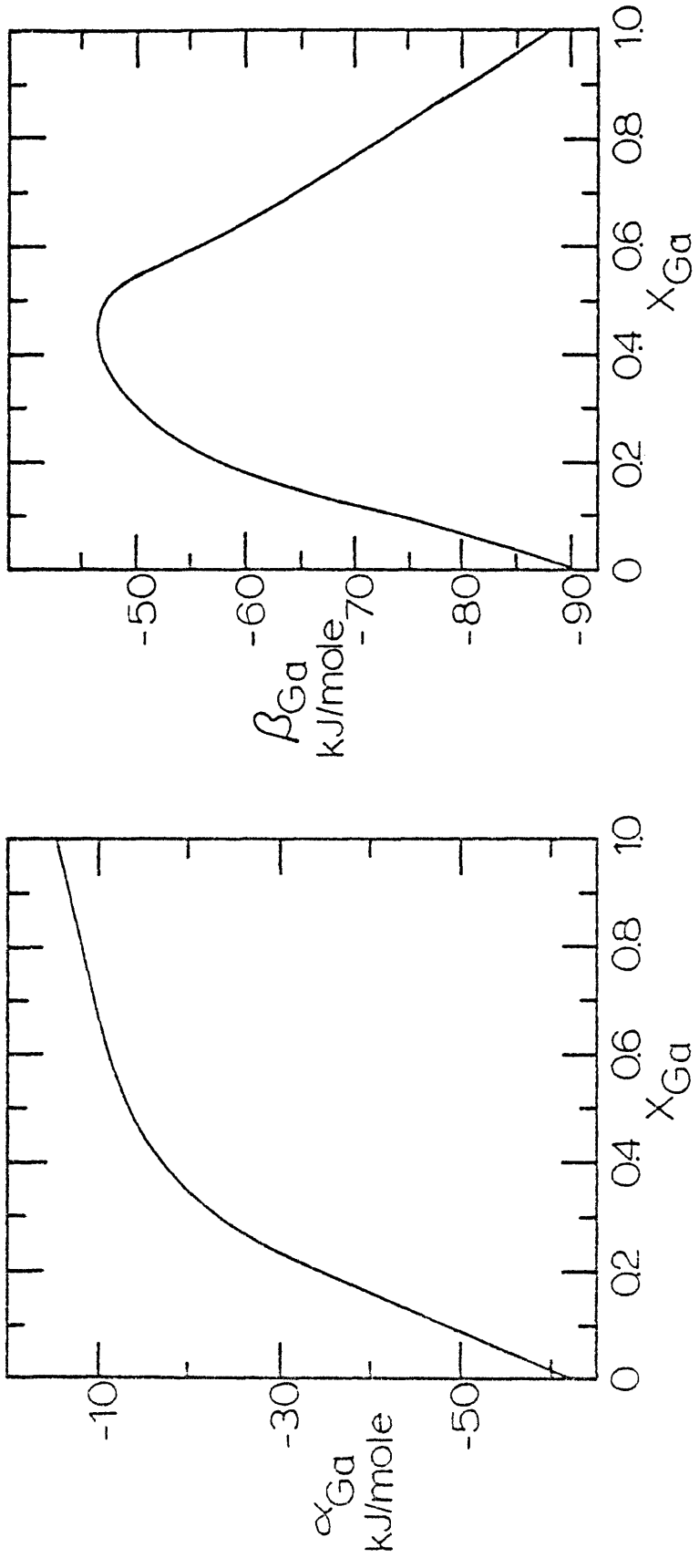

FIG. 16 - INTEGRATION PLOTS FOR THE LIQUID Cu-Ga SYSTEM AT 1500°K: (a) Ga ALPHA FUNCTION; (b) Ga BETA FUNCTION.

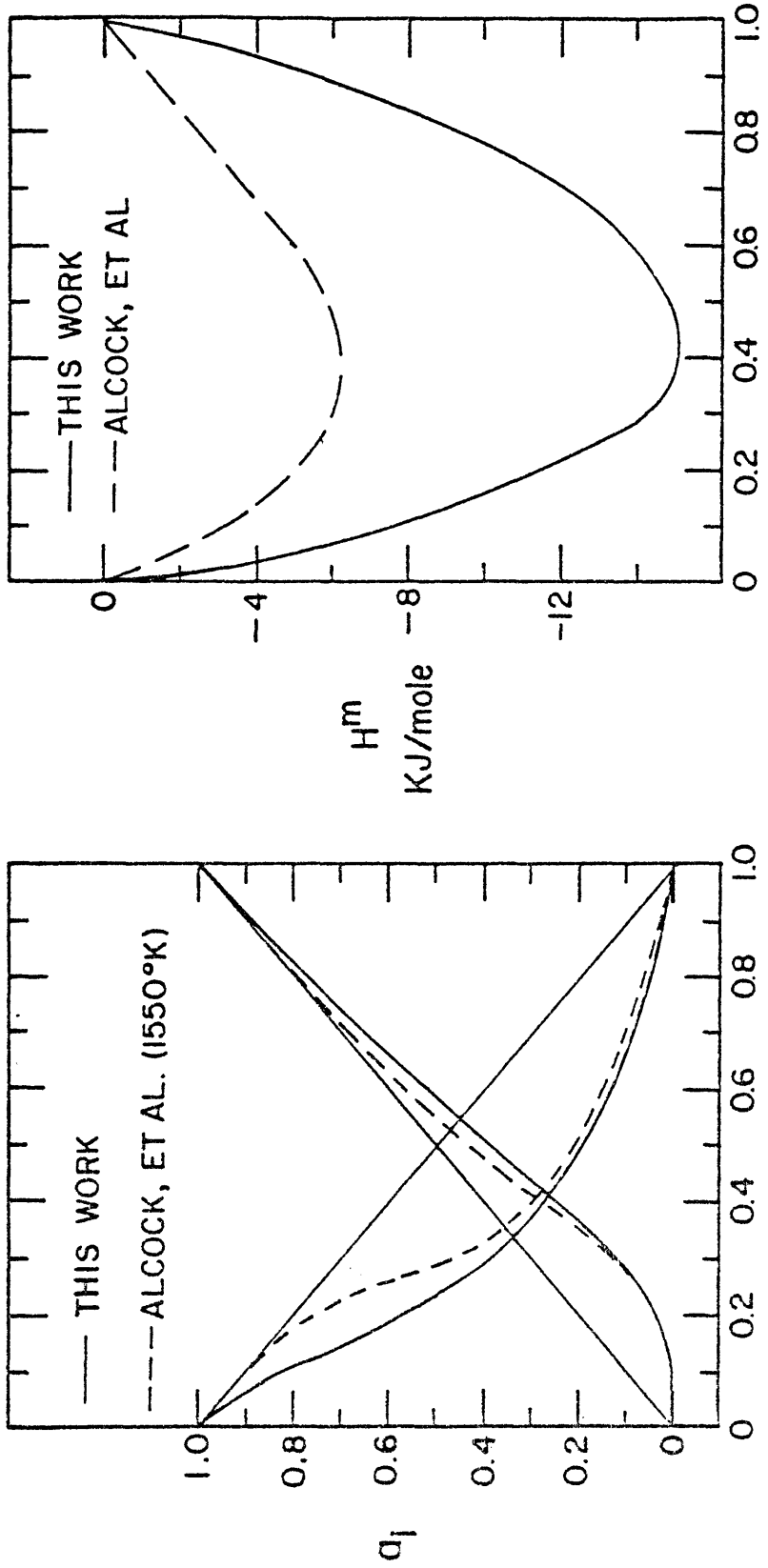

FIG. 17- SUMMARY OF RESULTS FOR THE LIQUID Cu-Ga SYSTEM AT 1500 °K: (a) ACTIVITIES; (b) INTEGRAL MOLAR HEAT OF MIXING.

TABLE V

RESULTS FOR THE LIQUID Cu-Ga SYSTEM AT 1500°K

X_{Ga}	a_{Ga}	γ_{Ga}	a_{Cu}	γ_{Cu}	H_{Ga}^{M} kJ/mole	H_{Cu}^{M} kJ/mole
1.00	1.000	1.000	-	0.197	0	-63.82
0.90	0.895	0.994	0.022	0.220	-0.84	-48.15
0.80	0.779	0.974	0.049	0.245	-2.93	-36.00
0.70	0.653	0.933	0.083	0.277	-6.28	-27.15
0.60	0.520	0.867	0.128	0.320	-9.20	-21.31
0.50	0.382 (±0.011)	0.764 (±0.023)	0.185 (±0.006)	0.370 (±0.011)	-11.51 (±6)	-18.14 (±6)
0.40	0.249	0.623	0.263	0.438	-17.15	-13.53
0.30	0.126	0.420	0.379	0.541	-24.69	-9.91
0.20	0.036	0.180	0.573	0.716	-36.61	-5.53
0.10	0.0045	0.045	0.820	0.911	-59.41	-1.56
0.00	-	0.00073	1.000	1.000	-90.00	0

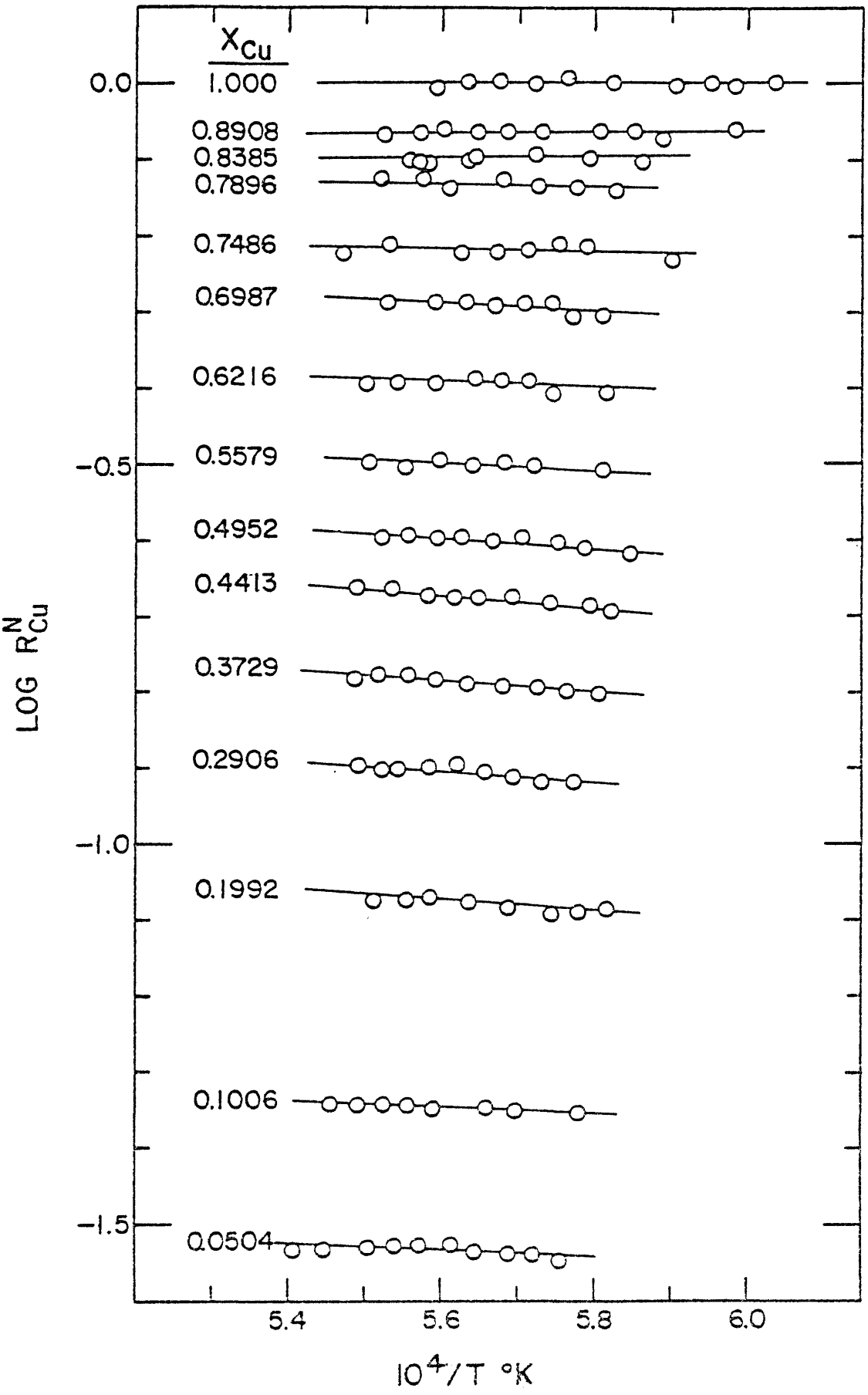

FIG. 18-NORMALIZED RELATIVE ION CURRENTS OF Cu FOR THE LIQUID Cu-Si SYSTEM.

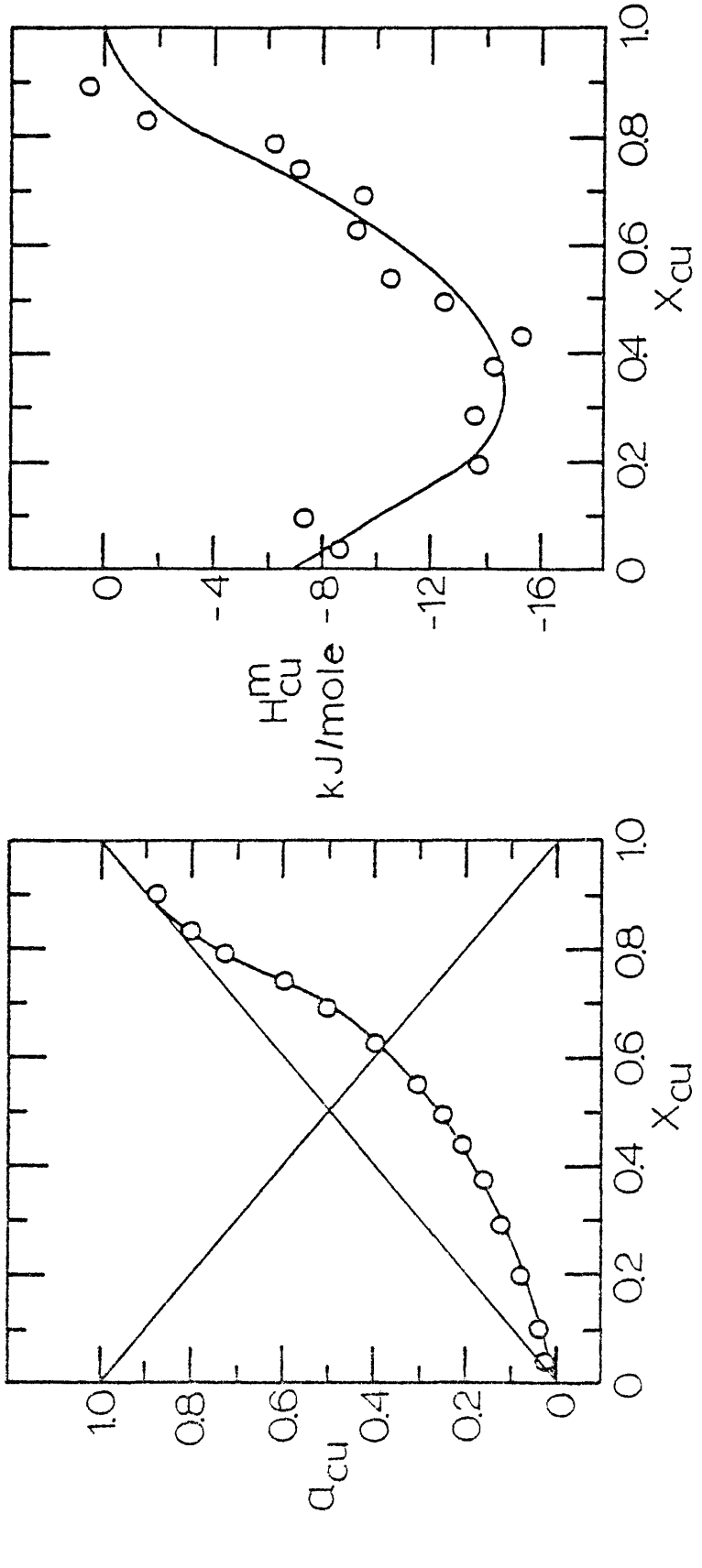

FIG.19– RESULTS FROM THE NORMALIZED RELATIVE ION CURRENT PLOT FOR THE LIQUID Cu-Si SYSTEM:(a) ACTIVITIES OF Cu AT 1750°K;(b) PARTIAL MOLAR HEATS OF MIXING OF Cu.

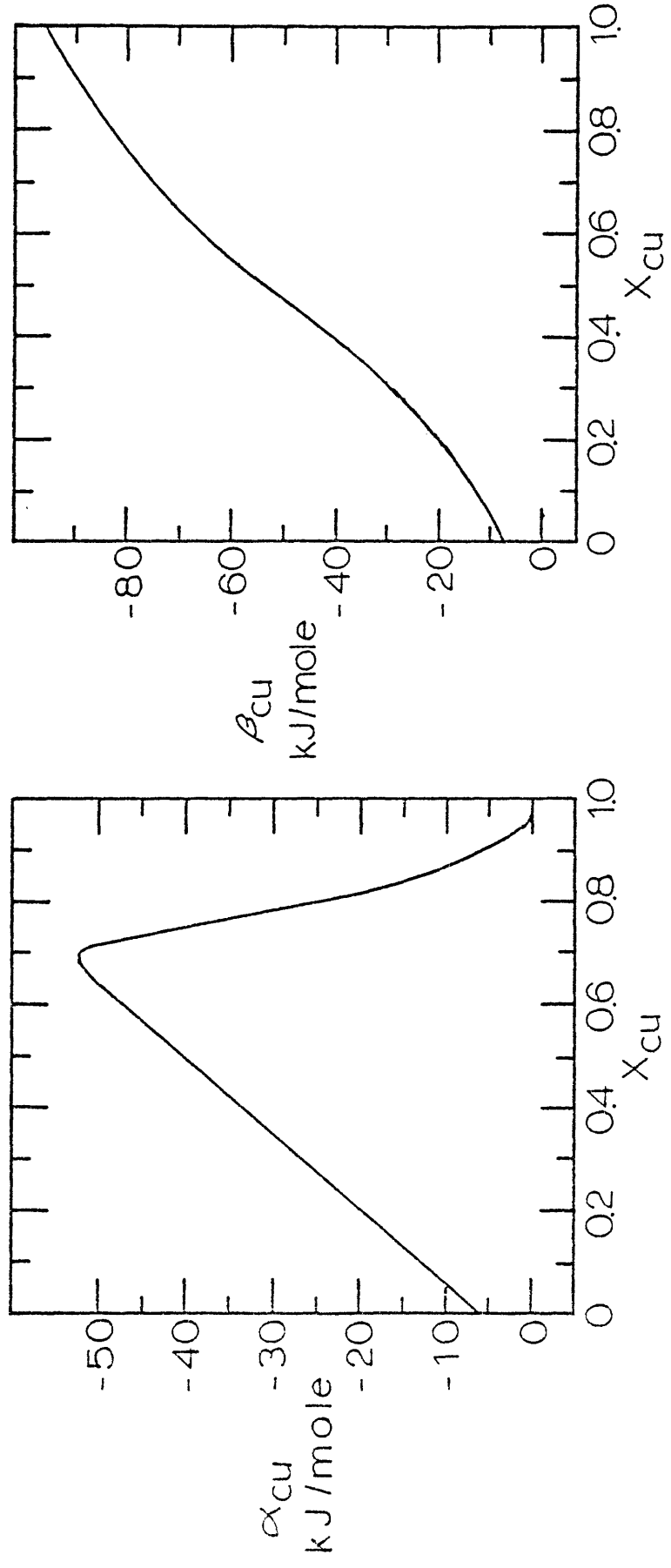

FIG. 20 - INTEGRATION PLOTS FOR THE LIQUID Cu-Si SYSTEM AT 1750°K: (a) Cu ALPHA FUNCTION; (b) Cu BETA FUNCTION.

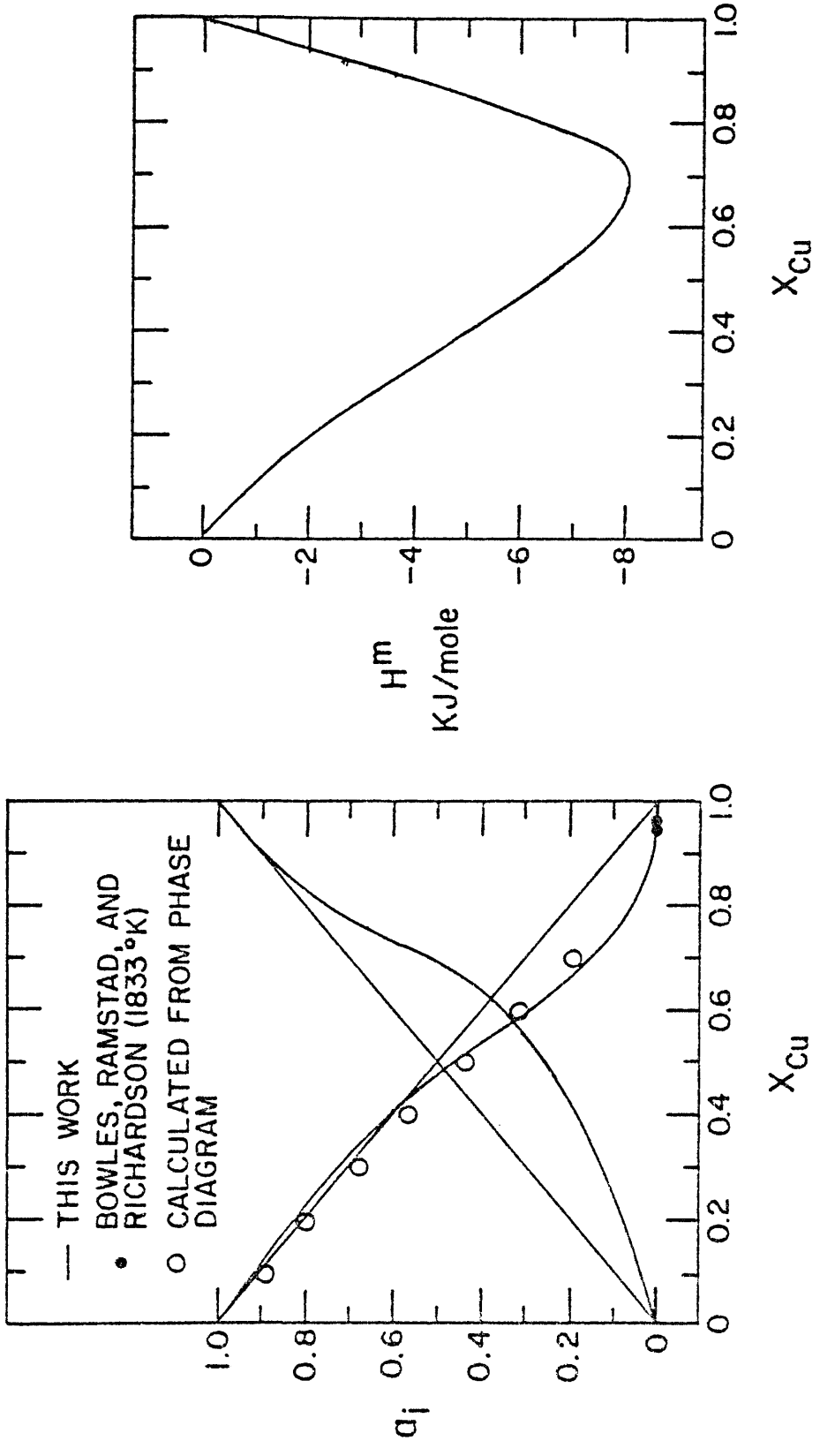

FIG. 21- SUMMARY OF RESULTS FOR THE LIQUID Cu-Si SYSTEM AT 1750 °K: (a) ACTIVITIES; (b) INTEGRAL MOLAR HEAT OF MIXING.

TABLE VI

RESULTS FOR THE LIQUID Cu-Si SYSTEM AT 1750°K

X_{Cu}	a_{Cu}	γ_{Cu}	a_{Si}	γ_{Si}	H_{Cu}^{M} kJ/mole	H_{Si}^{M} kJ/mole
1.00	1.000	1.000	-	0.156	0	-52.24
0.90	0.896	0.996	0.016	0.160	0.05	-34.84
0.80	0.750	0.938	0.046	0.230	-3.00	-20.89
0.70	0.498	0.711	0.152	0.507	-7.20	-10.21
0.60	0.348	0.580	0.294	0.735	-10.73	-3.04
0.50	0.251 (±0.008)	0.502 (±0.015)	0.452 (±0.014)	0.904 (±0.027)	-13.06 (±4)	-0.03 (±4)
0.40	0.177	0.443	0.606	1.010	-14.58	1.25
0.30	0.123	0.410	0.733	1.047	-14.41	1.19
0.20	0.078	0.390	0.832	1.040	-12.54	0.59
0.10	0.040	0.400	0.913	1.014	-9.80	0.13
0.00	-	0.669	1.000	1.000	-7.03	0

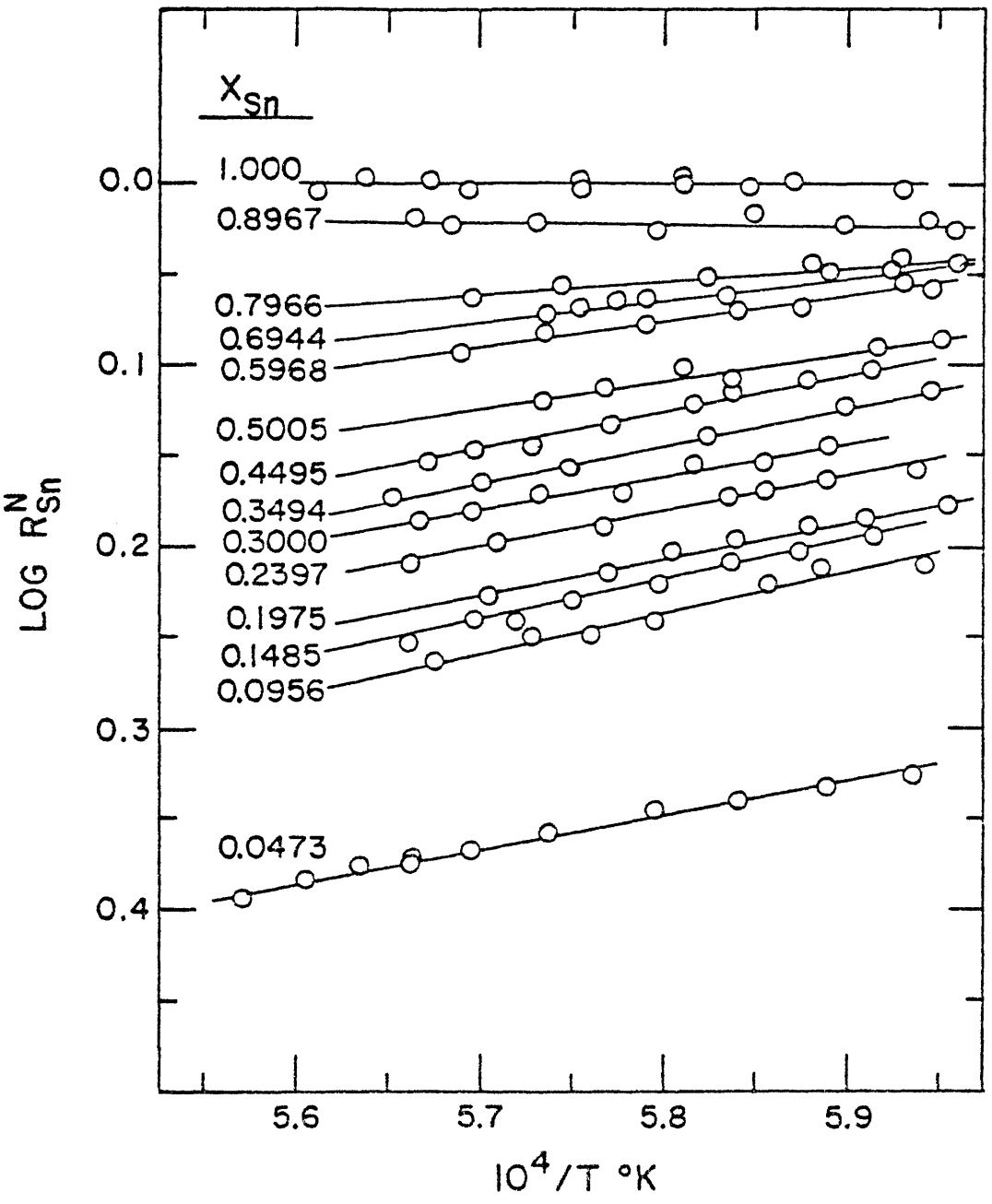

FIG. 22-NORMALIZED RELATIVE ION CURRENTS OF Sn FOR THE LIQUID Sn-Si SYSTEM.

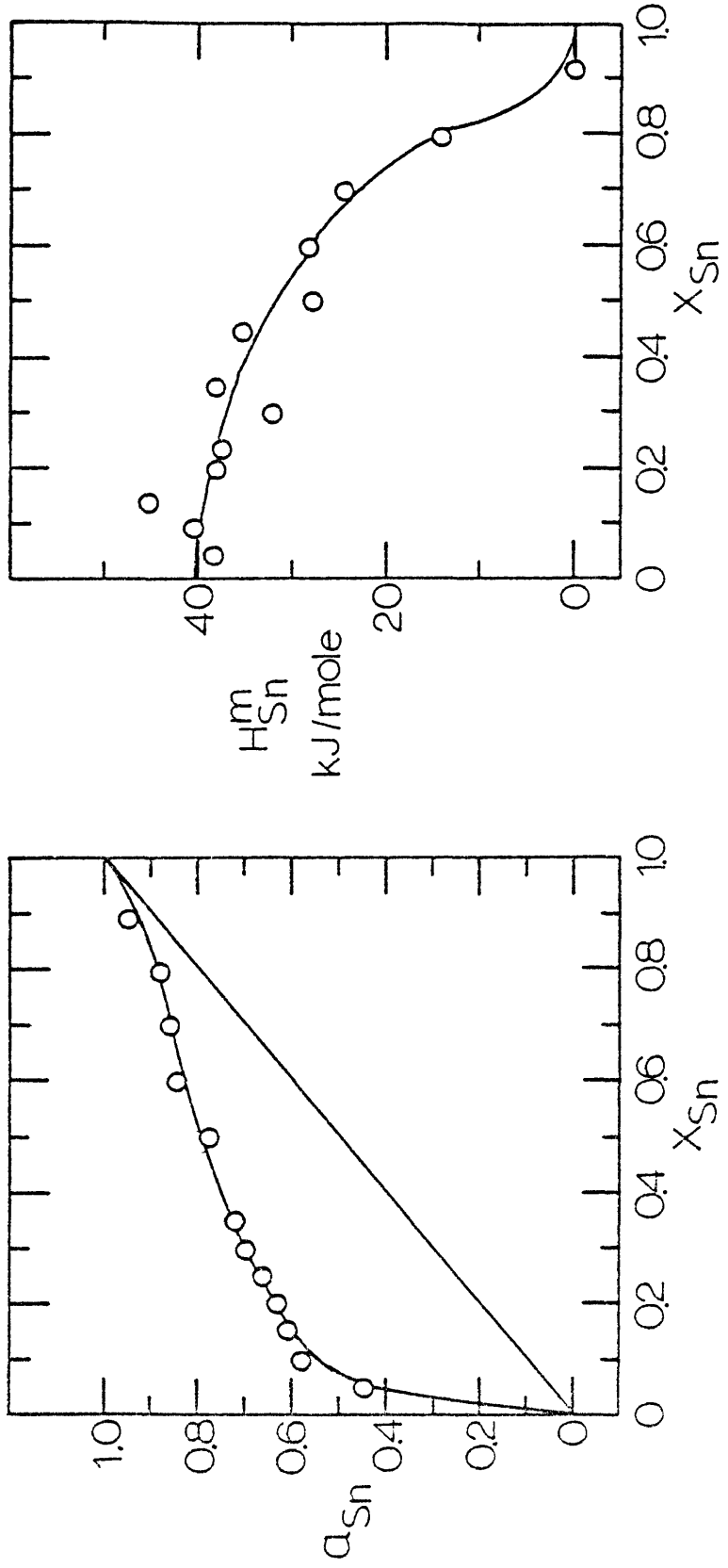

FIG. 23 - RESULTS FROM THE NORMALIZED RELATIVE ION CURRENT PLOT FOR THE LIQUID Sn-Si SYSTEM:(a) ACTIVITIES OF Sn AT 1723°K; (b) PARTIAL MOLAR HEATS OF MIXING OF Sn.

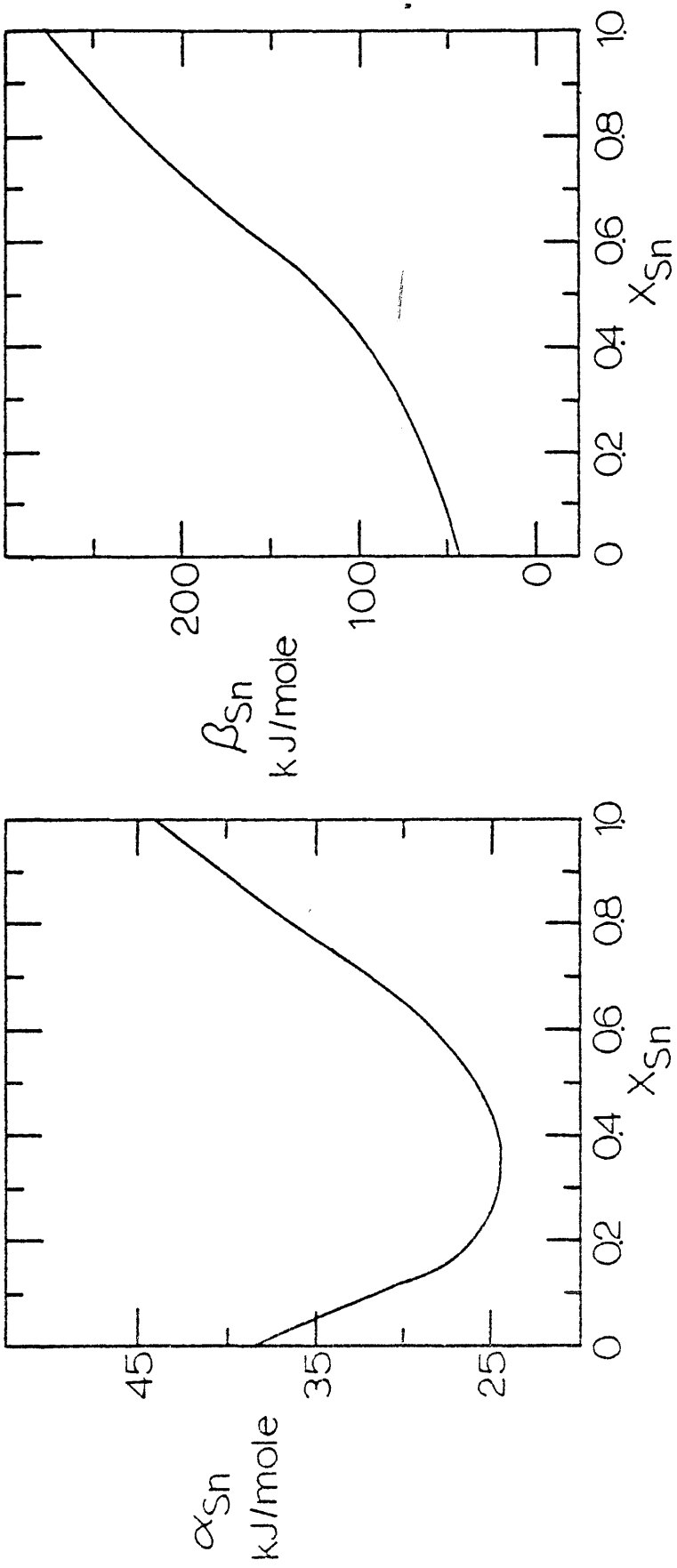

FIG. 24- INTEGRATION PLOTS FOR THE LIQUID Sn-Si SYSTEM AT 1723°K: (a) Sn ALPHA FUNCTION; (b) Sn BETA FUNCTION.

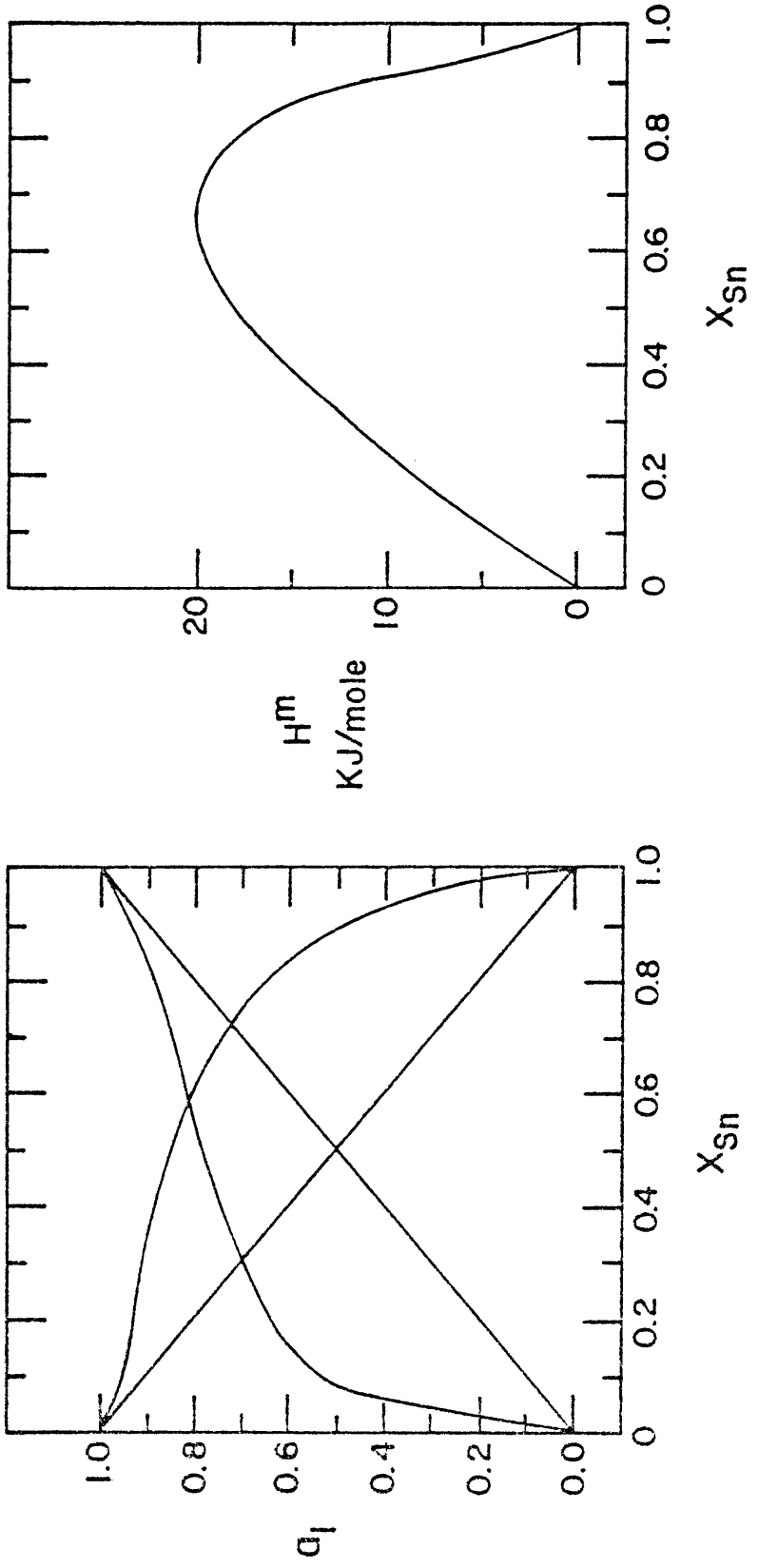

FIG.25-SUMMARY OF RESULTS FOR THE LIQUID Sn-Si SYSTEM AT 1723 °K:
(a) ACTIVITIE; (b) INTEGRAL MOLAR HEAT OF MIXING.

TABLE VII

RESULTS FOR THE LIQUID Sn-Si SYSTEM AT 1723^{o}K

X_{Sn}	a_{Sn}	γ_{Sn}	a_{Si}	γ_{Si}	H_{Sn}^{M} kJ/mole	H_{Si}^{M} kJ/mole
1.00	1.000	1.000	-	6.494	0	111.88
0.90	0.940	1.044	0.505	5.050	2.47	89.66
0.80	0.898	1.123	0.666	3.330	8.58	54.52
0.70	0.857	1.224	0.737	2.457	18.41	24.90
0.60	0.820	1.367	0.796	1.990	24.77	12.76
0.50	0.785 (±0.024)	1.570 (±0.047)	0.843 (±0.025)	1.686 (±0.051)	29.71 (±4)	6.53 (±4)
0.40	0.745	1.863	0.877	1.462	33.47	3.35
0.30	0.698	2.327	0.908	1.297	36.82	1.46
0.20	0.640	3.200	0.937	1.171	39.33	0.59
0.10	0.570	5.700	0.943	1.048	41.84	0.13
0.00	-	14.994	1.000	1.000	43.93	0

VIII. DISCUSSION OF RESULTS

The relative ion current technique is very precise for the determination of activity as evidenced by the excellent agreement of the present values and those in the literature. The large discrepancies with the reported partial molar heats of mixing are principly due to the error in this technique.

Cu-In The activities of In are in excellent agreement with Jagannath and Ghosh [24], and Azakami and Yazawa [26]. The small differences in the activities of Cu for this system are due to the interpretation of the alpha function. Neither of the earlier studies extended beyond X_{Cu} greater than 0.8 due to the phase boundary present at this composition at the temperatures at which their measurements were made. As extensive measurements were made in this region by this author it is believed that these reported results are the more accurate.

The partial molar heats of mixing of In are in fair agreement with Yazawa and Itagaki [28] from X_{In} = 1.0 to 0.3. At compositions below this point (28) shows much smaller heats than are reported here. This discrepancy is magnified by the application of the beta function as evidenced by the intergral molar heats of mixing.

Cu-Ga The activities of the components of this system are in good agreement with those reported by Alcock, Sridhar, and Svedberg[30]. The discrepancy shown is within the error of the techniques used.

The intergral molar heats from the literature[30] show smaller negative deviations than those in this study. Although the differences are large it must be remembered that both investigations are reporting second law heats which typically show a large degree of error.

Attempts were made by this author to obtain ion intensities of Cu in order to duplicate Alcock, et.al.[30] measurements by the ion current ratio technique. Sufficient precision for this quantity at low Cu concentration could not be obtained. As described in chapter I, it is this difficulty which limits the application of the ion current ratio technique.

Cu-Si The activity values reported by Bowles, Ramstad, and Richardson[31] indicate a more negative deviation from ideality than this study. This difference is negligible when the error in the equilibrium constant for the reaction

$$H_2 + SiO_2 \rightleftarrows H_2O + SiO$$

used by (31) is considered. The activities of Si calculated from the liquidous line determined by Rudolfi[44] and the partial molar heats of mixing from this work compare favorably

with the values presented.

There are at present no reported values for the heats of mixing of this alloy system. It should be noted that the uncertainty of these results are smaller than those of the Cu-In and Cu-Ga system due to the use of the new electronics.

Sn-Si Although there is no literature value for comparison, the precision of the activity measurements is expected to be as good as that demonstrated for the previously discussed systems. Due to the limited nature of the phase diagram as compiled by Hansen[45] only qualitative conclusions can be made. The system exhibits very low soluability which is indicative of the large positive deviation demonstrated in both the activities and intergral molar heats of mixing.

IX. CONCLUSIONS

The relative ion current technique has been demonstrated to be a precise means of activity determinations. This method's applicability to systems whose components have orders of magnitude differences in vapor pressures, allows the investigation of numerous new systems by Knudsen cell-mass spectrometry. The amenability of this technique to the study of limited composition ranges makes it ideal for infinite dilution investigations. Furthermore, this method can be used for the studies of multicomponent systems without additional complication of the equations and procedure.

The determined second law heats of mixing contain a significant degree of uncertainty. The reduction of this uncertainty requires extensive measurements for each alloy which for a specific system may not be practical.

The activity values of the liquid alloys studied showed excellent agreement with the available literature values. The error of these quantities is less than five percent.

The partial and integral molar heats of mixing measured disagreed significantly with that in the literature. The errors of these quantities are of the order of 4 to 6 kJ/mole.

Future application of the relative ion current technique

is suggested for two general areas. The first area of study is the measurement of activities for undefined systems. This work includes study over the complete or limited composition ranges of binary and multicomponent systems.

The second area of study suggested is the checking of previous investigations. Using this technique spot checks can be performed quickly and accurately for the numerous systems for which the present literature values show large discrepancies. In this manner the confidence in these reported results can be increased.

The following are lists of some of the systems which the author feels require further work and which may be studied using the relative ion current technique.

Al - Fe
Al - Pb
Al - Si
Al - Cu
Au - Fe
Fe - Cu
Cu - Fe
Cu - Ni
Fe - Mo (Dilute Mo)
Fe - Sn
Sn - Sb

Al - Cu - Si
Fe - Cr - Si
Fe - Ni - Si

APPENDIX I

Alpha and Beta Functions

The alpha and beta functions are used to calculate the activity and partial molar heat of mixing for one component of an alloy when these quantities are known for all other components of the alloy [6,15]. The definitions for these terms are

$$\alpha_i = \frac{RT \ln \gamma_i}{(1-X_i)^2}$$

$$\beta_i = \frac{H_i^M}{(1-X_i)^2}$$

The equations in which these terms are used for a binary system are as follows.

$$RT \ln \gamma_2 = -\alpha_1 X_1 X_2 - \int_{X_1=0}^{X_1} \alpha_1 \, d X_2$$

$$H_2^M = -\beta_1 X_1 X_2 - \int_{X_1=0}^{X_1} \beta_1 \, d X_2$$

The difficulty in the application of these functions is the

instability of α_i and β_i as $X_i \rightarrow 1$. Error in determinations of the γ_i and H_i^M causes a large degree of scatter in the plots of the defined functions in this composition region. This scatter may produce even larger errors in the calculated quantities due to the necessity of constructing a somewhat arbitrary line through this region.

APPENDIX II

Formulation of Equation For Heat of Vaporization Measurements

The equation used for these determinations is derived from the application of the Gibbs-Helmholtz equation

$$\frac{d(G/T)}{d(1/T)} = H \qquad \text{(AII-1)}$$

to the vaporization reaction

$$M(\text{liquid}) = M(\text{Vapor}) .$$

The standard free energy of this reaction is

$$G_v^o = -RT \ln a_m^{vapor} = -RT \ln P_m \qquad \text{(AII-2)}$$

where

a_m^{liquid} = 1 as the liquid is pure metal

P_m = vapor pressure of the metal.

Substitution of equation AII-2 into equation AII-1 gives the expression

$$\frac{d(\ln P_m)}{d(1/T)} = - \frac{H_v^o}{R}$$

Further substitution for P_m by equation I-10 results in the expression

$$\frac{d(\ln K R_m^+ T)}{d(1/T)} = - \frac{H_v^o}{R}$$

which upon integration becomes the final equation

$$\ln(R_m^+ T) = - \frac{H_v^o}{R} \left(\frac{1}{T}\right) + K' \qquad \text{(AII-3)}$$

Thus the slope of the line from the plot of $\ln(R_m^+ T)$ against $(1/T)$ yields the heat of vaporization.

APPENDIX III

Formulation of Relative Ion Current Equation for Polymer Species

For an alloy system where polymer species exist in sufficient quantities to produce error in the monomer measurements, the intensity of the polymer may be used in the determinations of activity and partial molar heats of mixing instead of the monomer.

$$x\ A\ (ALLOY) \rightleftarrows A_x\ (GAS) \qquad (AIII\text{-}1)$$

The standard Gibbs free energy change for the above reaction is

$$\Delta G^{O} = -RT \ln P_{A_x}/a_A^x$$

$$\ln P_{A_x} = -\frac{\Delta G^{O}}{RT} + x \ln a_A$$

Using the relationship of the Gibbs free energy, enthalpy, and entropy for reaction AIII-1, and relative partial molar quantities the following expressions can be formulated.

$$\text{ALLOY:}\quad \ln R^{+}_{A_x} = \left(\frac{-\Delta H^{O} + xH_A^M}{R}\right)\left(\frac{1}{T}\right) - \ln T + C'$$

$$\text{Pure A:} \quad \ln R^{+}_{A_x} = \frac{-\Delta H^{o}}{R}\left(\frac{1}{T}\right) - \ln T + C''$$

The difference of the above equations is the linear function with respect to 1/T for the normalized relative ion current.

$$\ln R^{N}_{A_x} = \frac{xH^{M}_{A}}{R}\left(\frac{1}{T}\right) + C$$

The activity is determined by the following equation.

$$a_A = (R^{N}_{A_x})^{\frac{1}{x}}$$

REFERENCES

1. Raychaudhuri, P.K., and Stafford, Science and Engineering, v. 20, p. 1-18 (1975).
2. Howard, S.M., The Mass Spectrometric Measurement of the Thermodynamic Properties of Liquid Metallic Solutions, PhD. Dissertation, Colorado School of Mines, 1971.
3. Howard, S.M., private communication, Colorado School of Mines, 1971.
4. Denbigh, K., The Principles of Chemical Equilibrium, London, Cambridge, 1966.
5. Wagner, C., Thermodynamics of Alloys, Reading Mass., Addison-Wesley Publishing Co., Inc., 1952.
6. Darken, L.S. and Gurry, R.W., Physical Chemistry of Metals, New York, McGraw-Hill, 1953.
7. Rapp, R.A., ed., Physicochemical Measurements in Metals Research, New York, Interscience Publishers, v. IV, parts 1 & 2, 1970.
8. Pehlke, R.D., Unit Processes of Extractive Metallurgy, New York, American Elsevier Publishing Company, 1973.
9. Darken, L.S., Trans. TMS-AIME, v. 239, pp. 80-89, 1967.
10. Orr, R.L., Trans. TMS-AIME, v. 236, pp. 1445-1450.
11. Spencer, P.J., Pool, M.J., Trans. TMS-AIME, v. 242, pp. 291-295, 1968.

12. Shen, S.S., Spencer, P.J., Pool. M.J., Trans. TMS-AIME, v. 245, pp. 603-606, 1969.

13. Hardy, H.K., Acta Met., v. 1, pp. 202-209, 1953.

14. Lupis, C.P.H., Elliot, J.F., Acta Met., v. 15, pp. 265-276, 1967.

15. Kubaschewski, O., Evans, E.LL., and Alcock, C.B., Metallurgical Thermochemistry, New York, Pergamon Press, 1967.

16. Lyubimov, A.P., Zobers, L., Rakhovski, V., Zh. Fiz. Khim., v. 32, pp. 1804-18108, 1958.

17. Belton, G.R., Fruchan, R.J., Hour. Phys. Chem., v. 71, pp. 1403-1409. 1967.

18. Margrave, J.L., ed., The Characterization of High Temperature Vapors, New York, John Wiley and Sons, 1967.

19. Moore, W.J., Physical Chemistry, 3rd ed., Englewood Cliffs, N.J., Prentice-Hall Inc., 1962.

20. Bird, R.B., Stewart, W.E., Lightfoot, E.N., Transport Phenomena, New York, John Wiley and Sons, 1960.

21. Jones, J.H., A Mass Spectrometric Investigation of the Thermodynamic Properties of the Liquid Gold-Copper and Gold-Germanium Systems, (Ph.D. Dissertation, Colorado School of Mines, 1969).

22. Barnard, G.P., Modern Mass Spectrometry. London, Institute of Physics, 1953.

23. Inghram, M.G., Hyden, R.J., and Hess, D.C., National Bureau of Standards, Circular 522, pp. 257-273, 1953.

24. Jagannathan, K.P. and Ghosh, A., Trans. Indian Inst. of Metals, v. 27, no. 5, pp. 298-302, 1974.

25. Hultgren, R., Orr, R.L., Anderson, P.D.,and Kelly, K.K., Supplement to the Selected Values of the Thermodynamic Properties of Metals and Alloys, New York, John Wiley and Sons, 1963.

26. Azakami, T. and Yazawa, A., Jour. Min. Met. Inst. Jap., v. 85, p.97, 1969.

27. Kleppa, O., Jour. Phys. Chem., v. 60, pp. 852-858, 1956.

28. Itagaki, K. and Yazawa, A., Jour. Jap. Inst. Met., v. 35, pp.389, 1971.

29. Hultgren, R. and Desai, P.D., Selected Thermodynamic Values and Phase Diagrams for Copper and Some of the Binary Alloys, INCRA Series on Metallurgy of Copper, 1971.

30. Alcock, C.B., Sridhar, R., and Svedberg, R.C., Jour. Chem. Thermodynamics, v. 2, pp. 255-263, 1970.

31. Bowles, P.J., Ramstad, H.F., and Richardson, F.D., Jour. Iron and Steel Inst., v. 202, pp. 113-121, 1964.

32. Baird, D.C., Experimentation: An Introduction to Measurement and Experiment Design, Englewood Cliffs, N.J., Prentice-Hall Inc., 1962.

33. Hager, J.P., Wilkomirsky, I.A., Trans. TMS-AIME, v. 242, pp. 183-189, 1968.

34. Hager, J.P., Walker, R.A., Trans TMS-AIME, v. 245, pp. 2307-2312, 1969.

35. Hager, J.P., Howard, S.M., Jones, J.H., Met. Trans., v. 1,

pp. 415-422, 1970.

36. Kiser, R.W., Introduction to Mass Spectrometry and its Application, Englewood Cliffs, N.J., Prentice - Hall, Inc., 1965.

37. Wiley, W.C., Science, v. 124 , pp. 817-823, 1956.

38. Winterbloom, W.L., Hirth, J.P., Jour. Chem. Phys., v. 37, pp.784-793, 1962.

39. Boyer, A.J., Meadcrowft, T.R., Trans. TMS-AIME, v. 233, pp. 388-391, 1965.

40. Hager, J.P., Howard, S.M., and Jones, J.H., Trans. TMS-AIME, v. 4, pp. 2383-2388, 1973.

41. Inghram, M.G. and Dowart, J., Proceedings of an International Symposium on High Temperature Technology, New York, McGraw-Hill Book Co., pp. 219-240, 1960.

42. Dowart, J. and Honig, R.E., Jour. Phys. Chem, v. 61, pp.980-985, 1957.

43. Natrella, M.G., Experimental Statistics, National Bureau of Standards Handbook 91, Washington, D.C., 1966

44. Rudolfi, E., Z. Anorg. Chem., v. 53, pp. 216-227, 1907.

45. Hansen, M., Constitution of Binary Alloys, 2nd ed., New York, McGraw-Hill Book Co., Inc., 1958.

BIOGRAPHICAL NOTE

The author was born in Iola, Kansas, on July 19, 1949. He attended the Denver Public school system and graduated from Denver-South High School in June 1967. In 1971 a B.A. in Chemistry was earned by the author from The John Hopkins University in Baltimore, Maryland. He is a member of the American Institute for Mining, Metallurgy, and Petroleum Engineers (AIME), the Society of Sigma Xi, and the Tau Episilon Phi Social Fraternity.

The author's parents, Joseph L. and Theresa W. Blattner, and family reside in Denver, Colorado.